Synthetic ion channels and pores (2004–2005)

Adam L. Sisson,[a] Muhammad Raza Shah,[b] Sheshanath Bhosale[a] and Stefan Matile*[a]

Received 13th February 2006
First published as an Advance Article on the web 18th May 2006
DOI: 10.1039/b512423a

This *critical review* covers synthetic ion channels and pores created between January 2004 and December 2005 comprehensively. The discussion of a rich collection of structural motifs may particularly appeal to organic, biological, supramolecular and polymer chemists. Functions addressed include ion selectivity and molecular recognition, as well as responsiveness to light, heat, voltage and membrane composition. The practical applications involved concern certain topics in medicinal chemistry (antibiotics, drug delivery), catalysis and sensing. An introduction to principles and methods is provided for the non-specialist; some new sources of inspiration from fields beyond chemistry are highlighted.

1 Introduction

"Synthetic ion channels and pores" are compounds that (a) have abiotic scaffolds (*i.e.*, scaffolds that are not found in biological ion channels and pores) and (b) act in lipid bilayer membranes.[1] This definition excludes ion channels and pores formed by *de novo* peptides, chemically modified or bioengineered membrane proteins and peptides, or natural products. Porous artificial membranes and pores formed in materials other than bilayer membranes are not covered either. The difference between ion channels and pores is that the former mediate the translocation of inorganic ions only, whereas the latter also transport molecules across bilayer membranes. Their mechanism of transport differs from carriers and transporters on the one hand and detergents, fusogens, and endovesiculators on the other. Unlike the former, ion channels and pores do not move significantly during transport. Unlike the latter, ion channels and pores do not disturb the structure of the lipid bilayer significantly. To avoid overemphasis of mechanistic considerations, it is always helpful to recall that classical ion carriers and detergents like valinomycin and triton X-100, respectively, can behave like ion channels under appropriate conditions.

This introductory section continues with a summary, as concise as possible, of the fundamental principles and methods in the field. Readers familiar with the topic are encouraged to move directly to either the following section, offering a more subjective primer on new sources of inspiration from related fields, or directly to the main topic covered in section 3. Readers interested in a more detailed description of principles and methods will find the references needed at the end of this section.

As far as the characterization of synthetic ion channels and pores is concerned, planar bilayer conductance experiments as well as fluorescence and Na NMR translocation assays in vesicles are the most common methods. The occurrence of single channel currents in planar bilayer conductance experiments is often considered as the hallmark of ion channels and pores. Adaptable and compatible with structural studies,

[a]*Department of Organic Chemistry, University of Geneva, Geneva, Switzerland. E-mail: stefan.matile@chiorg.unige.ch; Fax: +41 22 379 5123; Tel: +41 22 379 6523*
[b]*HEJ Research Institute of Chemistry, International Center for Chemical Sciences, University of Karachi, Karachi-75270, Pakistan*

Adam Sisson

Adam Sisson graduated with an MChem from the University of Sheffield (UK) in 2001 before moving on to gain a PhD from the University of Bristol (UK) in 2005. His PhD was spent in the group of Professor A. P. Davis synthesising and studying steroid derived receptors for anions as transmembrane transporters. His research interests are in supramolecular chemistry applied within the lipid bilayer environment and he is currently pursuing these interests as a post-doc in the group of Professor S. Matile in Geneva.

Muhammad Raza Shah

Muhammad Raza Shah was born at Charsadda, Pakistan in 1976. He carried out his PhD (2003) work at the Max-Planck Research Institute for Polymer Research in Mainz, Germany, in the group of Professor Adelheid Godt. He spent one year in the group of Professor Stefan Matile as a post-doc at Geneva University, Switzerland. Currently he is Assistant Professor at the HEJ Research Institute of Chemistry, University of Karachi. His research interests are at the interface of synthetic organic chemistry, supramolecular chemistry and materials chemistry, focusing on interlocked molecules and artificial ion channels.

fluorescence translocation assays in multilabeled spherical bilayers (*i.e.*, vesicles or liposomes) can, however, be preferable to reliably determine the key characteristics of current topics of interest. Na NMR flux assays are often used for the direct observation of sodium transport, often avoided for the elaboration of key characteristics, and incompatible with pores.

Key characteristics of synthetic ion channels and pores include size, ion and membrane selectivity, pH, voltage and ligand gating, and blockage. Different from ohmic or voltage insensitive ion channels, non-ohmic ion channels violate Ohm's law and are described by their gating charge z_g. Changes in partitioning account in most cases for voltage sensitivity, rectification is usually negligible. Important expressions of remote control of ion channel activity, by the surrounding membrane, beyond voltage gating, include membrane composition, fluidity, thickness, stress and surface potential. Bell-shaped dependence on membrane thickness is used to identify hydrophobic matching in support of transmembrane active structures. Dependence on membrane fluidity is sometimes evoked to discriminate between mobile carriers and immobile channels. This interpretation as such is erroneous because changes in partitioning are usually dominant. Dependence on membrane composition and surface charge are of interest for medicinal applications.

Hill profiles describe the dependence of pore activity on the n-th power of the monomer concentration. Hill coefficients $n > 1$ reveal both stoichiometry and instability of active supramolecules, $n = 1$ identifies either active monomers or stable supramolecules of unknown stoichiometry and $n < 1$ interference by inactive supramolecules. In single channel conductance experiments thermodynamic instability ($n > 1$) is observed as a low, and stability ($n \leqslant 1$) as a high, probability P_0 to observe open channels. Kinetic lability is reflected in short, and inertness in long, single channel lifetimes τ.

The inner diameter of ion channels and pores can be determined by size exclusion experiments. Quantitative values are accessible from single channel conductance. The Hille model is directly applicable to high-conducting pores (1–5 nS); correction factors for low-conducting ion channels (1–100 pS) are available. Saturation behavior due to blockage by permeant ions requires extrapolation to low ionic strength.

Anion/cation selectivity describes the overall preference of synthetic ion channels or pores for anions or cations, selectivity sequences or topologies their preferences among anions and cations. Permeability ratios are calculated from the reversal potential V_r with the Goldman–Hodgkin–Katz (GHK) equation or approximated from flux rates in vesicles. Selectivity sequences derived from permeability ratios and conductance, describing the ability of ions to enter and move through channels, respectively, can differ. Classical classifications such as Eisenman topologies I–XI for group I cations and halide topologies I–VII compare dehydration penalty with energy gains from ion binding in the channel. The least interesting and most frequent situation is pure dehydration (Eisenman I, $Cs^+ > Rb^+ > K^+ > Na^+ > Li^+$; halide I, $I^- > Br^- > Cl^- > F^-$, historically referred to as Hofmeister or lyotropic sequence). Sequences IV are relevant concerning biological potassium and chloride channels. Transmembrane proton and electron transport are of interest with regard to bioenergetics and photosynthesis.

The subtle shift from ion selectivity to blockage by the permeant ion is detected as saturation behavior with increasing electrolyte (salt) concentration and best described by inhibitory concentration IC_{50} (or the apparent dissociation constant K_D) and the maximal conductance g_{MAX}. Multiple binding of ions or molecules for selective hopping provides access to selectivity without blockage.

Molecular recognition by synthetic multifunctional pores is the key to applications like sensing and catalysis. The response to chemical stimulation is ligand gating or blockage. Dose–response curves reveal effective (EC_{50}) and inhibitory concentrations (IC_{50}) for ligand gating and blockage, respectively. They depend on many parameters such as pH, ionic strength, self-assembly, membrane potential, ion selectivity, and so on. The Hill coefficient n can reflect the number of ligands or blockers. Available methods for the stochastic detection of molecular recognition and transformation in single channel

Sheshanath Bhosale

Sheshanath Bhosale was born in 1976 in Indral Latur, India. He received his MSc from SRTM, University Nanded, India in 1999. He then moved to the Freie University Berlin, Germany, where he received his doctoral degree in supramolecular chemistry under the supervision of Professor J. H. Fuhrhop in 2004. He moved to the University of Geneva, Switzerland, for a post-doc under the supervision of Professor S. Matile in March 2005. His research is focused on the design and synthesis of artificial photosystems. Recently he obtained a 'Roche Fellowship'.

Stefan Matile

Stefan Matile received his Diploma (1989) and PhD (1994) from the University of Zurich under the direction of Wolf Woggon. After a post-doc with Koji Nakanishi at Columbia University, New York (1994–1996) and three years as Assistant Professor at Georgetown University, Washington DC, he moved to the University of Geneva (1999), where he is currently Full Professor in the Department of Organic Chemistry. His research interests are at the interface of synthetic organic, biological and supramolecular chemistry; current emphasis is on multifunctional nanoarchitecture in lipid bilayer membranes.

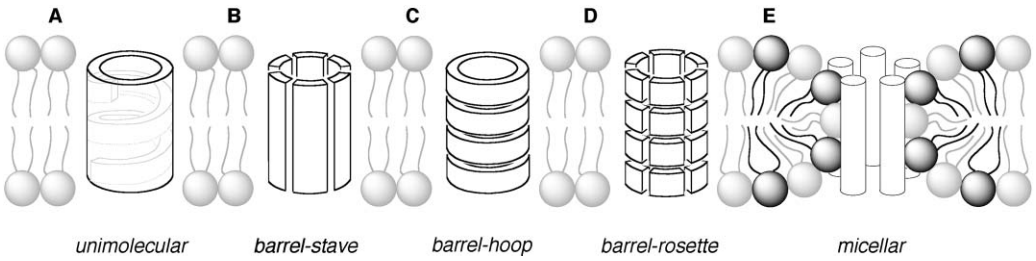

Fig. 1 Classical motifs in the field of synthetic ion channels and pores are (A) unimolecular macromolecules, often foldamers, (B) barrel-stave and (C) ''barrel-hoop'' supramolecules as well as the more complex (D) ''barrel-rosette'' and (E) micellar pores.

measurements remain to be applied to synthetic ion channels and pores. The voltage dependence (V) of molecular recognition by synthetic ion channels and pores (K_D) is described in the Woodhull equation. Woodhull distances, l_w, from pore entrance to active site, reveal the depth of molecular recognition (and confirm that blockage indeed takes place in the membrane). Applied to catalysis, voltage dependence can be expressed in steering factors for substrate binding and product release.

The above principles and methods for the characterization of synthetic ion channels and pores will be described elsewhere in more detail;[2] accounts on selected topics such as polarized vesicles[3] and ion selectivity in vesicles[4] are already available. We reiterate that the definitions and terms elaborated in this introduction are highly simplified, do not intend to be generally valid or to question, invalidate or exclude other views of the topic. They are made for convenience with the only intention to assist reading of this review by the non-specialist.

In research that focuses on the creation of function, evidence for the desired function is naturally all that really matters. Reconfirmation of the validity of the structural information used to create this function deserves lower priority. It is not further problematic in this context that the arguably most useful $n > 1$ ion channels and pores are undetectable on the structural level. Any structural classification of synthetic ion channels and pores remains, therefore, at least in part speculative. Classical and expected motifs include barrel-stave, barrel-hoop, barrel-rosette and micellar supramolecules (Fig. 1).

2 New sources of inspiration

Several inspiring breakthroughs during the last two years in membrane protein crystallography, natural product chemistry, membrane biotechnology and membrane biophysics concern aromatic rings positioned either at the inner or at the outer surface of biological or bioengineered ion channels and pores. Internal aromatic rings are known from the pioneering potassium channel structure to account, not for the expected potassium selectivity, but for blockage by tetraethylammonium cations. This motif reappears in what is arguably the crystal structure of the years 2004–2005, that is, the AmtB ammonia channel of *Escherichia coli* (Fig. 2A).[5] An important nutrient for bacteria, the aromatic ring is found at the channel mouth to recruit the ammonium cations from the environment by cation–π interactions. The $pK_a \sim 9$ of the dehydrated ammonium cation is then lowered, and the neutral gas is guided through the hydrophobic channel by hydrogen-bonding histidines. This elegant acid–base chemistry is introduced

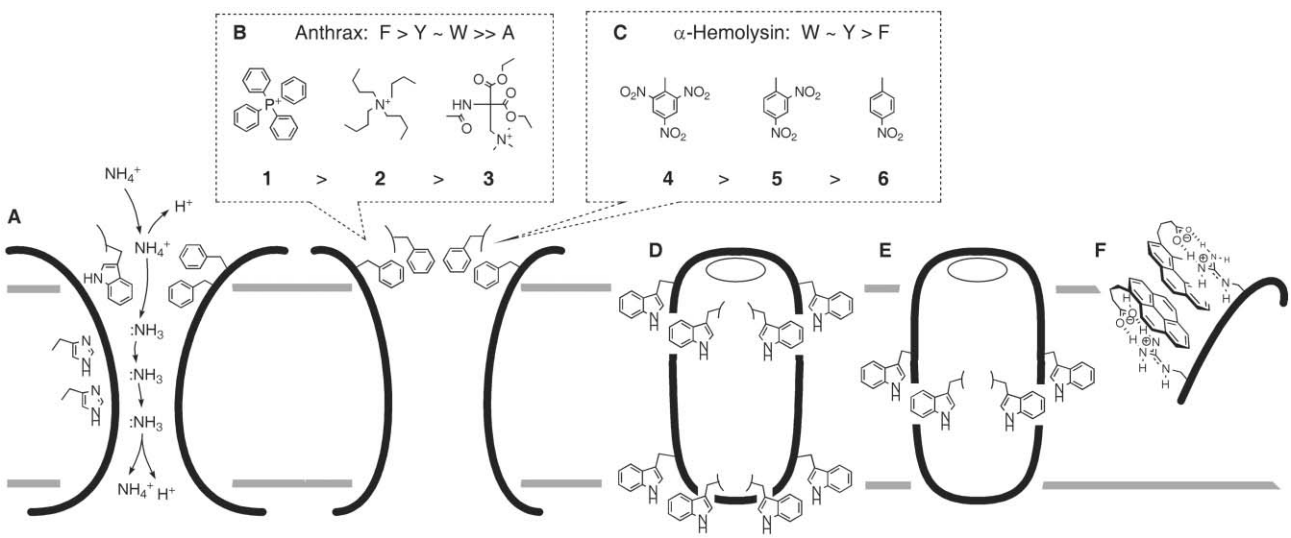

Fig. 2 Internal and external aromatic rings (A) as an ammonium trap in the ammonia channel, (B) as protein translocators in the anthrax pore with cation–π blockers **1–3**, (C) engineered into the α-hemolysin pore for TNT sensing, (D) in favorable and (E) in unfavorable external positions for protein translocation and anchoring, and (F) higher aromatics as activators of arginine-rich cell-penetrating peptides for arene-templated ion pairing and facilitated translocation.

to assure ammonium selectivity, that is, to prevent the transport of inorganic cations like potassium. Methylammonium cations are transported as well, ethylammonium and dimethylammonium cations are blockers, and larger amines and ammonium cations are inactive.

Internal π-clamps mediate protein translocation through the anthrax pore (Fig. 2B).[6] Namely, cysteine scanning revealed that phenylalanine (F) residues define the most narrow part of the pore. Their replacement by the smaller alanine (A) increases the conductance of the pore but hinders rather than helps protein translocation through the pore. 35 ammonium and phosphonium cations were tested as blockers of the anthrax pore. Aryl phosphoniums like **1** were best (K_D = 46 nM), alkylammoniums like **2** intermediate, and hydrophilic ammoniums like **3** only weakly recognized. Blockage by hydrophobic cations decreased slightly with tryptophan (W) and tyrosine (Y) rings and dramatically with alanine (A) rings (**1**: K_D = 1.7 mM). These results suggest that internal π-clamps play an active role in protein translocation by non-specifically interacting with hydrophobic areas of unfolded proteins, thereby preventing protein refolding during translocation.

Nearly identical internal π-clamps were engineered into the α-hemolysin pore for stochastic sensing of the explosive 2,4,6-trinitrotoluene (TNT) **4** (Fig. 2C).[7] Increasing, very weak dissociation constants with increasing electron density of the π-clamps (W ~ Y > F) as well as decreasing electron density in 2,4-dinitrotoluene (2,4-DNT) **5** (K_D = 3.2 M) and 4-nitrotoluene (4-NT) **6** (32 M) were in support of aromatic electron donor–acceptor interactions. The discrepancy of expected and found pore blockage and an overall poor sensitivity were interpreted as indications that blockage does not take place as designed. TNT sensing was selected as representative illustration of much progress with bioengineered ion channels and pores because of compatibility with the theme of aromatic rings. Other studies covering light-switchable potassium channels and mechanosensitive pores or the detection of the growth of a single polymer chain have been summarized elsewhere.[8]

The aromatic rings frequently found at outer rather than inner surfaces of biological ion channels and pores are famous for their preferred location at the membrane–water interface (Fig. 2D). This interfacial preference of external aromatics is thought to facilitate insertion, translocation and positioning of ion channels and pores in biomembranes. During 2004–2005, energy scales for partitioning that include positional information became available.[9] The key innovation was to bypass the phase transfer across the hydrophobic core, that complicates comparative studies, by one-sided addition to the bilayer. This was achieved using lateral ejection of model helices from the translocon into the bilayer membrane. The translocon is the switching station next to the ribosome that directs newly synthesized, unfolded proteins either into or across the membrane. The big surprise was that the partitioning of some (the electron-rich, H-bond donating W, Y and H) but not all overall hydrophobic aromatics (F) into the hydrophobic core is energetically unfavorable (Fig. 2E). For the design of new, and the interpretation of results with old, synthetic ion channels and pores,[1] this means that certain central external rings will destabilize rather than stabilize active structures (Fig. 2E). These aromatic surprises may further explain why aromatic carboxylates like pyrenebutyrate catalyze the translocation of arginine-rich cell-penetrating peptides across bilayer membranes (Fig. 2F).[10]

The positioning of external aromatic rings is a fine example for key contributions by the surrounding bilayer to the structure and activity of ion channels and pores that are missed in studies in bulk membranes and in the solid state. Arguably the most impressive example reported in 2004–2005 for lipid bilayers contributing to pore function concerns the lantibiotic nisin.[11,12] This food preservative is a ribosome-synthesized, post-translationally modified peptide characterized by five intramolecular rings formed by the rare thioether amino acids lanthionine and 3-methyllanthionine. Reminiscent of the classical barrel-stave channel formed by amphotericin B together with ergosterol, nisin acts as an antibiotic by targeted pore formation with lipid II. Structural studies with pyrene-labeled cell-wall precursor lipid II suggest that the active pore is a dodecamer composed of eight nisins and four lipids II. In conductance experiments in planar diphytanoylphosphatidylcholine (DiPyPC) bilayers, lipid II reduces the threshold voltage of the ohmic nisin pore from −100 mV to −5 mV, increases the single channel lifetime from milliseconds to 6 seconds and the pore diameter from 1 nm to 2.0–2.5 nm.

The newly identified ion channels formed by the proapoptotic triterpene avicin **7** also include lipids from the surrounding membrane into the active structure (Fig. 3).[13] Hill analysis of the concentration dependence implies a decameric pore, poly(ethylene glycol) (PEG) size exclusion experiments a diameter of 1.1 nm. Removal of the amphiphilic side chain A annihilates ion channel activity; small modifications produce cholesterol sensitivity. These findings suggest that only this side chain A inserts into the membrane and forms the dodecameric channels. No ion selectivity in neutral, but conductance-independent cation selectivity in anionic, membranes (P_{K^+}:P_{Cl^-} = 5:1) demonstrated inclusion of lipids into the active suprastructure.

As far as pores and porous materials unrelated to lipid bilayer membranes are concerned, one of the key breakthroughs from 2004–2005 is that, with tetramer **8**, coordination barrel-stave supramolecules are now long enough to span a bilayer membrane and stable enough to exist without internal templates such as **9–11**.[14] As for the previously discussed[1] π-stacked, ionophoric supramolecular rosettes such as guanine quartets,[15,16] the appearance of Fujita–Stang architecture in synthetic ion channels and pores is only a matter of time.

Among the most exciting pores engineered into stable polymers (rather than unstable lipid bilayers) are conical gold pores **12–15** and terminally functionalized cylindrical carbon nanotube pores **16–18**.[17,18] Conical gold pores are attractive because the preparation by electrolytic plating of edged pores provides straightforward access to small diameters. Their asymmetry provides access to a characteristic that has been studied extensively with several synthetic ion channels and pores in lipid bilayer membranes since about 1998, *i.e.*, non-ohmic behavior.[1,19–24] Their internal gold surface allows the positioning of functional groups such as anionic carboxylates (**12**) and cationic ammoniums (**13**), and molecular recognition

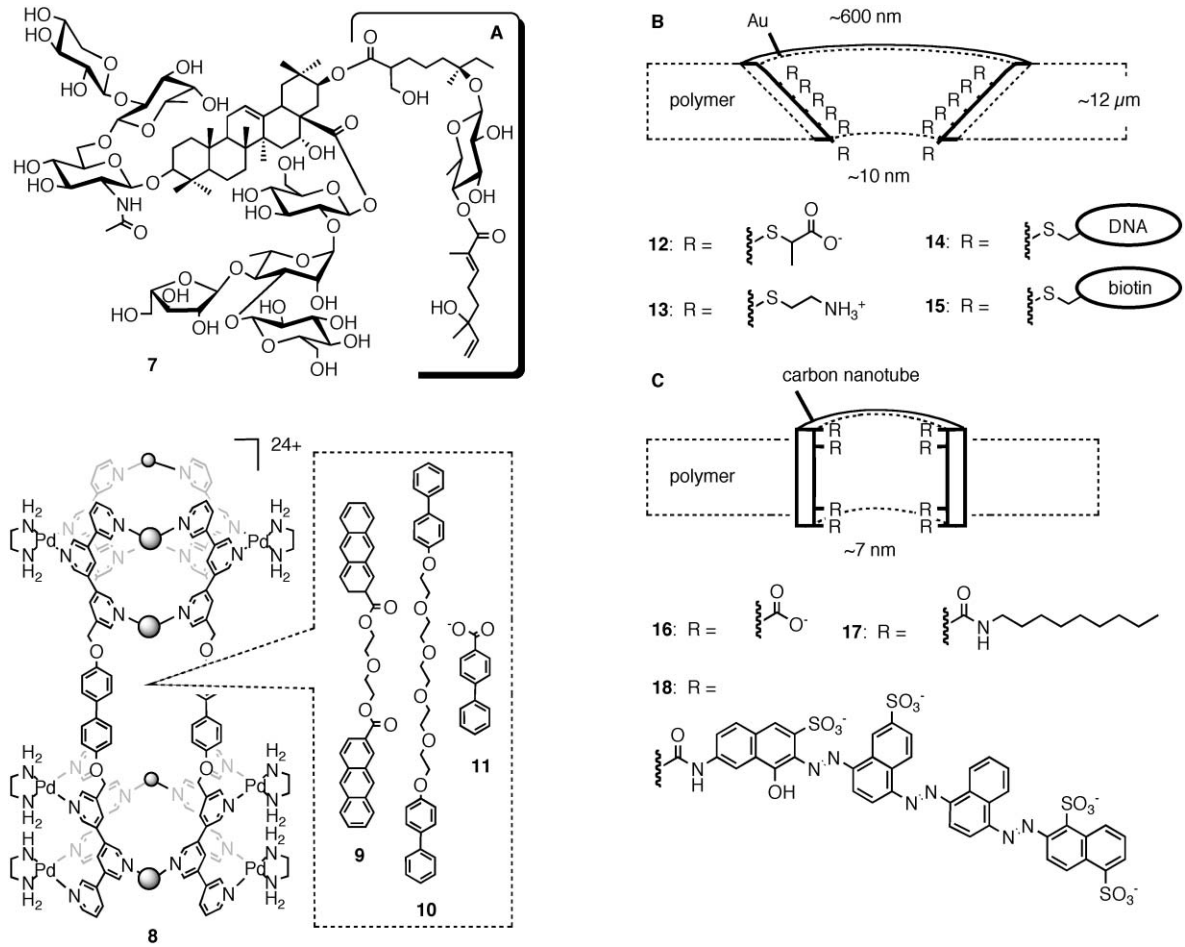

Fig. 3 Avicin **7**, a representative new source of inspiration from natural product chemistry (A: essential for function), barrel-stave architecture **8** with guests **9–11** as a representative new source of inspiration from supramolecular coordination chemistry, and multifunctional gold (B) and carbon nanotube (C) pores in polymer membranes as representative new sources of inspiration from materials sciences.

units such as DNA (**14**, several sequences), biotin (**15**), protein-G and an antiricin antibody. Reproducing extensive insights from synthetic ion channels and pores in lipid bilayer membranes since 2000,[1,25–27] the authors find that the functionalized pores can be specifically blocked with the corresponding guests, *i.e.*, streptavidin, immunoglobulin G, and ricin.

In an alternative approach, cylindrical carbon nanotube pores **16–18** could be positioned vertically in polymer membranes and functionalized by reacting the terminal carboxylates (**16**) with amines of various size, hydrophilicity and charge (*e.g.* **17** and **18**).[28,29] With these membranes, it was possible to measure the frictionless water flux through the smooth, repellant carbon nanotubes. The found velocities (10–44 cm s^{-1}) were four to five orders of magnitude faster than expected from conventional fluid-flow theory, comparable with that through aquaporin water channels, and only slightly faster than hexane (6 cm s^{-1}). Terminal functionalization resulted in cation flux that increased with increasing negative charge and decreasing ionic strength (**18** > **16** > **17**). Size selectivity increased with decreasing hydrophobicity and inner diameter.

These examples of new sources of inspiration were selected subjectively. They are also meant to highlight the interdisciplinary nature of the field of synthetic ion channels and pores, reaching from structural biology and membrane biophysics to natural products, supramolecular coordination chemistry, materials science, nanotechnology, and so on. Highlighting our ability to create functional molecules from scratch at increasingly high levels of sophistication, the field remains, however, first of all a celebration of the power of modern synthetic organic chemistry.

3 Current synthetic ion channels and pores

This is the central section of this review, where synthetic ion channels and pores created between January 2004 and December 2005 are summarized comprehensively. We move from unimolecular and barrel-stave motifs to the more complex barrel-rosette and micellar systems (Fig. 1). General trends include a great revival of unimolecular approaches with a coinciding decline of stacked macrocycles. Barrel-rosette channels remain underexplored, whereas barrel-stave supramolecules continue to be the most advanced topic.

3.1 Non-peptide macrocycles

The cyclodextrin motif of the original Tabushi channel[30,1] reappeared in 2005. Different from the original "barrel-hoop"

approach, β-cyclodextrin **19** was designed to form a unimolecular anion channel (Fig. 4).[31] Oligoether tails were chosen as they are hydrophobic and long enough to span a lipid bilayer, and a ring of ammonium cations was positioned next to the cyclodextrin portal to select for anions. Despite these cations, highly facilitated Na^+ flux across egg yolk phosphatidylcholine (EYPC) vesicle membranes was observed using an NMR assay. However, a pH-sensitive fluorescent dye assay was modified to show that **19** exhibited anion selectivity regarding transport rates across vesicle membranes ($I^- > Br^- > Cl^-$). Cl^- and Na^+ were transported at a similar rate.

The hydrophobic thio-β-cyclodextrin **20** produced the appearance of single channel currents in planar asolectin bilayers.[32] Higher order cyclodextrin aggregates are thought to account for this activity.

Cucurbituril **21** (CB[6]), a macrocyclic cavitand with symmetric carbonyl fringed portals (diameter ~ 3.9 Å), was found to transport protons and alkali metal cations across EYPC vesicle membranes.[33] Fluorometric assays involving pH-sensitive dyes were employed. Proton flux mediated by **21** was effectively blocked in the presence of acetylcholine **22**, known to be a high affinity host for **21**. The found Eisenman I selectivity topology with distinct Li-anomaly was opposite to binding affinity ($Li^+ > Cs^+ \sim Rb^+ > K^+ > Na^+$, the contracted pentameric analog exhibited weak $Li^+ > Na^+$ with no transport of larger cations). In planar bilayer measurements with a Cs^+ electrolyte solution, CB[6] **21** exhibited short-lived, heterogeneous single-channel conductances in the range of gramicidin. Different from the axial tails on one face in most macrocyclic channels, including **19**, the alkyl tails in CB[6] **21** are equatorial. This unique topology is proposed to cause the formation of unimolecular channels with micellar domains in the bilayer.

Calix[4]arene–cholate conjugates **23–27** were tested for H^+ and Na^+ transport across PC/PG vesicle membranes using a pH-sensitive dye assay and a ^{23}Na NMR assay (Fig. 5, PC/PG: phosphatidylcholine (1,2-diacyl-*sn*-glycero-3-phosphocholine)/phosphatidylglycerol {1,2-diacyl-*sn*-glycero-3-[phospho-*rac*-(1-glycerol)]}).[34] The more active 1,3-alternate conformers **23–25** with axial cholate tails on both faces of the macrocycle are, at 35 Å long, long enough to span the bilayer. Linear concentration dependence supports a unimolecular mode of action. The cone conformers **26** and **27**, with axial cholate tails on only one face of the macrocycle, are shorter (~25 Å) and less active. The degree of acetylation within each series had only a marginal effect.

To create pH-sensitive ion channels, the pK_as of the bowl-shaped tetracyanoresorcin[4]arene **28** were lowered by introducing *ortho*-cyano groups as π-acceptors.[35] As expected for gradual resorcinol deprotonation, the single channel conductance in planar lipid bilayers increased with increasing pH from 6.0 to 8.5. A transmembrane tail-to-tail "barrel-hoop" dimer is postulated as the active structure with the pH-sensitive resorcinols as anionic portals. Voltage sensitivity at pH 8.5 was attributed to asymmetrically charged dimers.

Calix[4]resorcinarene **29**, with the unifacial axial azo dyes in the *trans*-configuration, exemplifies continuing[36–39,1] interest in photogating (compare section 3.3). It was designed to form dimeric barrel-hoop channels that can close in response to *cis–trans* photoisomerization.[40,41] In planar soybean lecithin bilayers, the *trans*-isomers **29** produced single channels with lifetimes in the millisecond range.

The most popular macrocycles remain crown ethers (Fig. 6). The ion channels formed by dibenzo-18-crown-6 disulfonate **30** in planar lipid bilayers exhibited an unexpected Eisenman I selectivity topology ($Cs^+ > Rb^+ > K^+ > Na^+ > Li^+$).[42] A

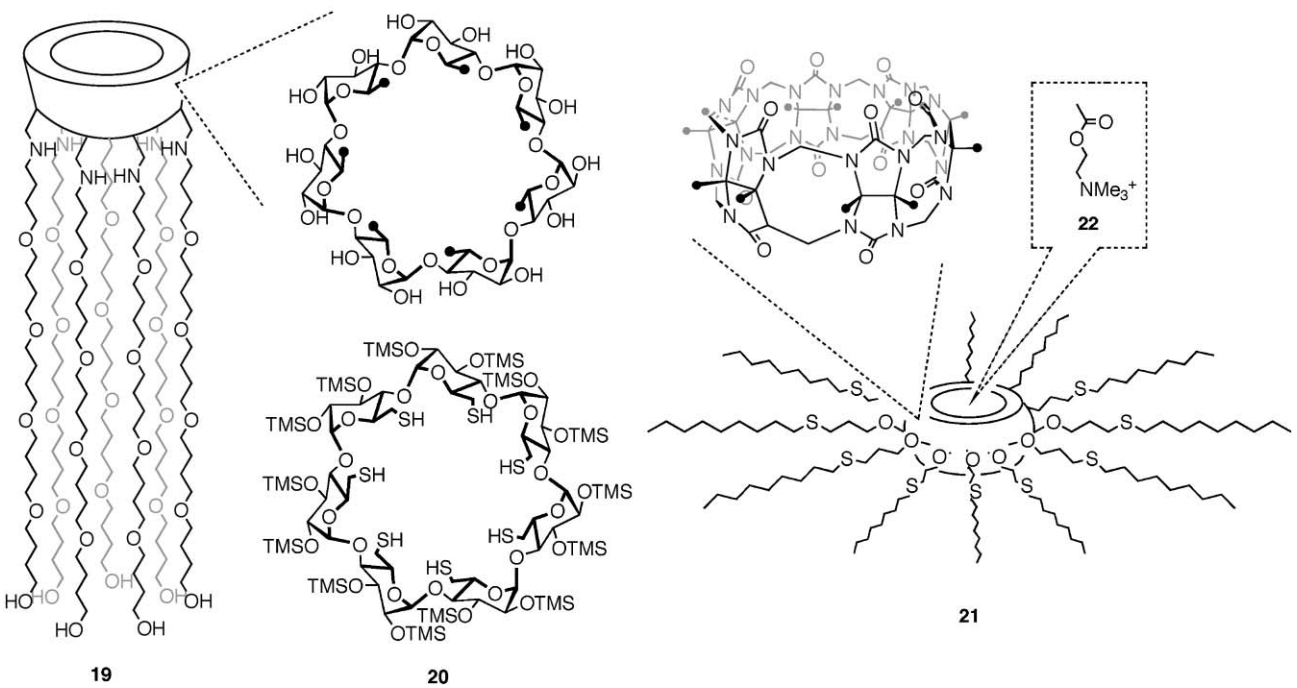

Fig. 4 Synthetic ion channels with cyclodextrin and cucurbituril macrocycles.

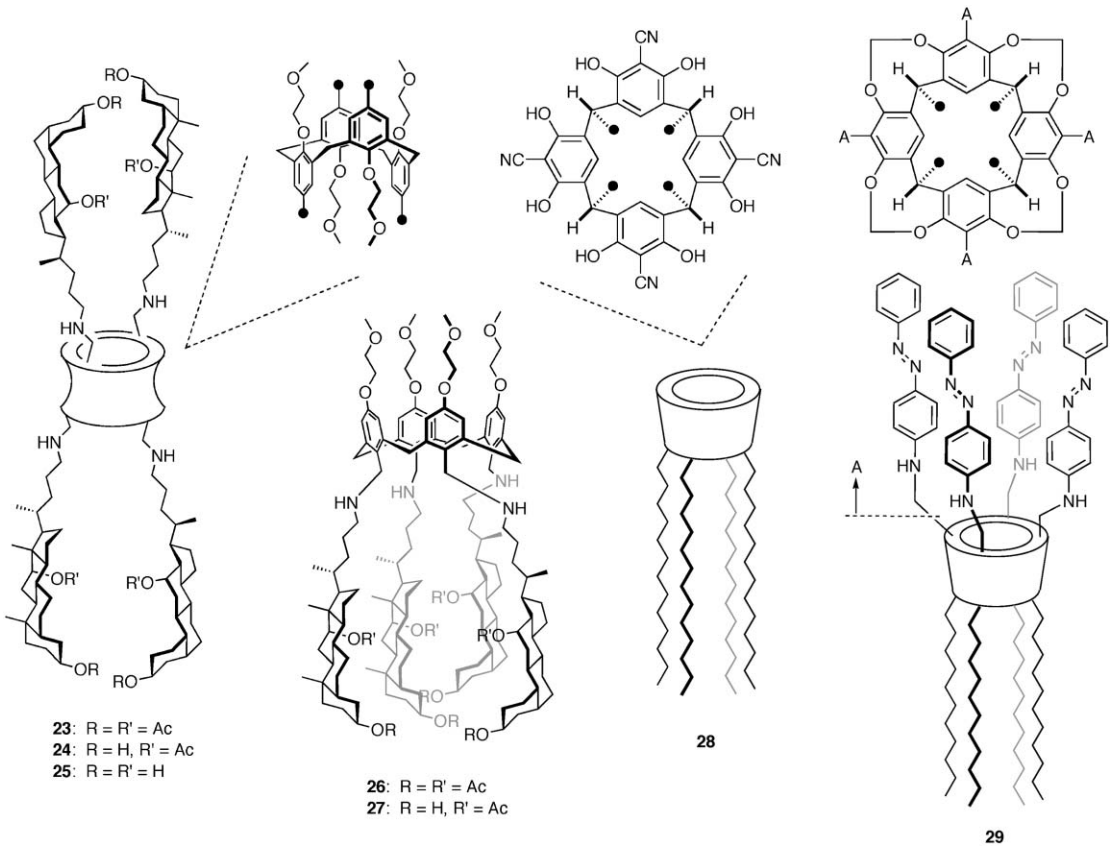

Fig. 5 Synthetic ion channels with macrocyclic oligoarenes.

supramolecular active structure with crowns plus sulfonates is thought to contribute to this obviously weak, dehydration-dominated cation binding.

Dialkyl-diazacrowns **31–36** were studied for Na^+ transport across dioleoyl (DOPC) and dipalmitoyl phosphatidylcholine (DPPC) vesicles, as well as for their antibacterial activity against Gram-positive and Gram-negative bacteria.[43] The shorter alkyl chain derivatives **31–33** showed faster transport rates and higher antibacterial activity. This length dependence was interpreted as suggestive of a carrier mechanism.

Oligocrowns **37–43** are part of one of the oldest family of synthetic cation channels.[1,44,45] Previous studies revealed a parabolic dependence of activity on the length of the spacer between the macrocycles, with maximal activity at hydrophobic matching of channel length and bilayer thickness.[1,45] General validity of hydrophobic matching for maximal activity of oligocrowns **37–43** has now been confirmed for dimyristoleoyl (DMPC), dioleoyl (DOPC) and dierucoyl phosphatidylcholine (DEPC) large unilamellar vesicles.[46] As expected for the membrane thickening effect, increasing cholesterol concentrations shifted the maximal activity in DMPC membranes to longer oligocrown channels. The antibacterial activities of oligocrowns **37–43** against Gram-negative *E. coli* and Gram-positive *Bacillus subtilis* cells showed identical parabolic length dependences; oligocrown **39** showed maximal activity.[47] Good agreements between antibacterial activities and Na^+ efflux rates from liposomes were also found for oligocrown analogs **44–53**.[48,49] Maximal bactericidal and hemolytic activities were found for **39** > **40** > **46**, with little selectivity between bacterial and mammalian cells. Bactericidal activities of oligocrowns **44–48** against *E. coli* decreased with decreasing pH from 7.1 to 5.5; protonation of the macrocyclic amino components would be expected to hinder cation transport.[50] A potential-sensitive fluorescent probe confirmed that rapid depolarization accounts for the toxicity of oligocrown channels. In whole cell patch clamp experiments on human embryonic kidney cells (HEK 293), oligocrown **49** caused an increase in membrane conductance. Currents evoked by addition of oligocrowns **40**, **44** and **48** were 3 to 4 times those resulting from activation of native glutamate channels with kainate.[51] By repeated rinsing of the extracellular medium, oligocrowns could be 'washed out' of the system, leaving vital cells with diminished residual conductivity. Formation and ion transport mechanism of oligocrown channels were simulated by course grain molecular modeling.[52–54]

Peptides **54–58** adopt α-helical conformations in a variety of media, including the hydrophobic lipid bilayers.[55] The rational positioning of modified crown ethers bearing amino acids gave a rod-like structure wherein the cation binding functionalities are aligned to create a transmembrane pore. Single channel experiments in planar DPPC bilayers demonstrated K^+ ion channel activity of **54**. According to dynamic ^{23}Na NMR kinetics and pH-stat experiments in PC/PG vesicles, activities of peptides **54–58** decreased with decreasing crown size. The crown-free phenylalanine-analog was inactive. Results of attenuated total reflectance infrared spectroscopy (ATR-IR) spectroscopy could be interpreted as a mixture of active helices in transmembrane orientation and inactive helices at the

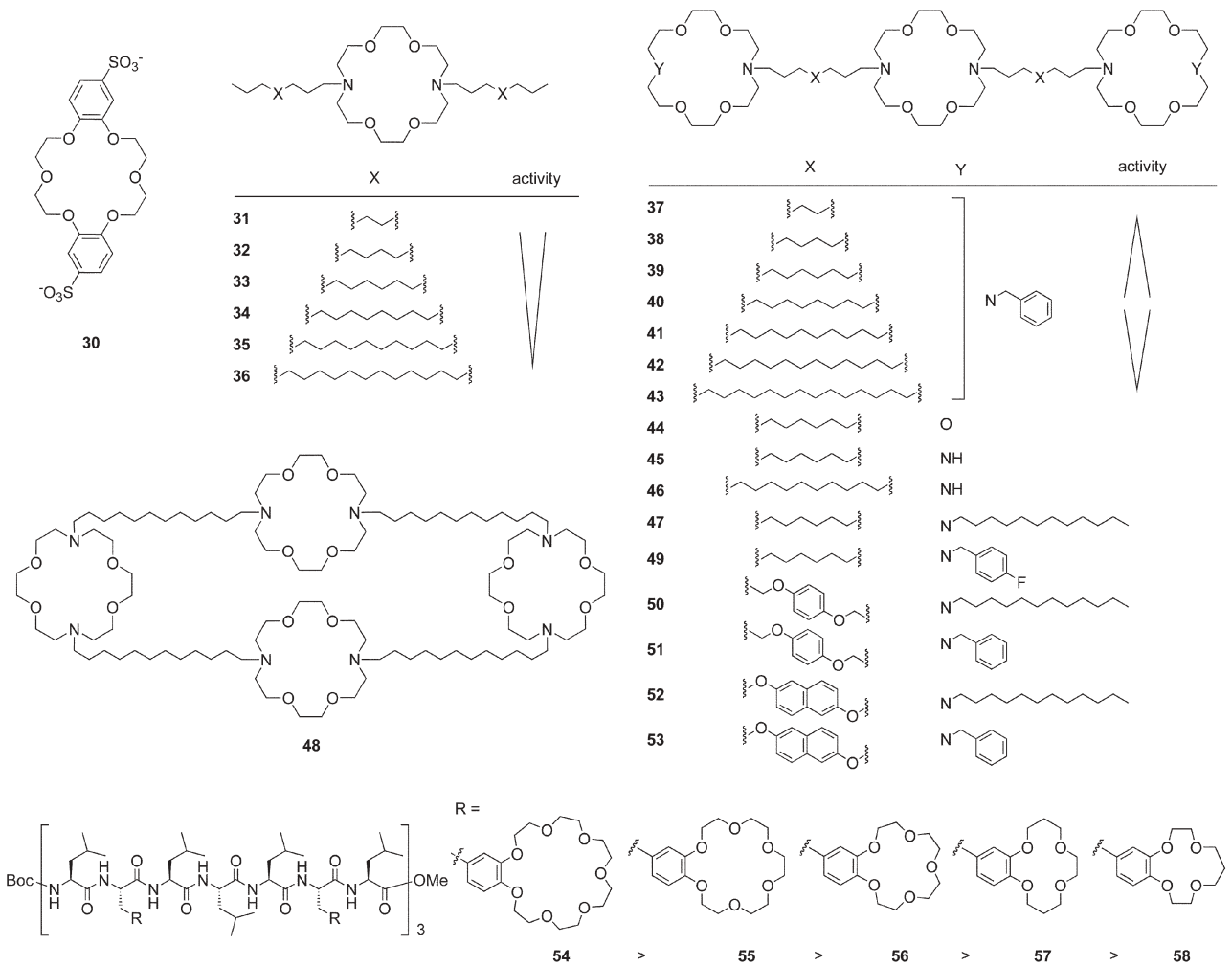

Fig. 6 Synthetic ion channels with oligocrown ionophores.

interface. Peptides **54** and **56** exhibited high cytotoxicity against breast cancer cells (MDA) and mouse leukaemia cells (P388).

3.2 Barrel-stave supramolecules

According to preliminary results from pH-sensitive fluorescent probes, the giant rigid-rod PEG macrocycle **59** is active in EYPC membranes (Fig. 7).[56] Similar activity of the acyclic analog **60** is in disagreement with the proposed active structure, a giant barrel-stave supramolecule characterized in detail in the solid state. Macrocycle **59** showed linear concentration dependence; diol **61** was inactive.

It is always easier to stop than to start a process. In the field of synthetic ion channels and pores, this common wisdom is reflected in the existence of several ion channels and pores that close in response to chemical stimulation (blockage),[1,25–27] whereas the complementary opening in response to chemical stimulation (ligand gating) persists as one of the big challenges in the field. To obtain access to ligand gating, the rigid-rod π-stack barrel-stave architecture was introduced.[57,58] Because of a hoop–stave mismatch, self-assembly of the *p*-octiphenyl **62** with electron-poor naphthalenediimides (NDIs) along the scaffold was expected to yield the twisted, closed π-helix **63** rather than an open barrel-stave ion channel. Compensation of the hoop–stave mismatch by highly cooperative (n = 6.5, EC_{50} = 13 μM) intercalation of the complementary dialkoxynaphthalene (DAN) donors **64** caused the expected helix–barrel transition and produced surprisingly homogenous, ohmic, low-conductance (expected: $d \approx 5$ Å, found: d_{Hille} = 3.5 Å; g = 94 pS) anion channels **65** (P_{Cl^-}/P_{K^+} = 1.38). Concerning selectivity, it was found that shortening of the alkylammonium tails in **62** and removal of the anionic head or hydrophobic tail in ligand **64** all cleanly annihilated ligand-gated ion channel formation; other intercalators like adenosine monophosphate (AMP) or guanosine monophosphate (GMP) were inactive. Helix–barrel transition as the origin of ligand gating was confirmed by silencing of the exciton coupled circular dichroism (CD) signature of the twisted NDI stacks in π-*M*-helix **63**, the presence of operational aromatic donor–acceptor interactions by the plum color of DAN–NDI charge transfer complexes in ion channel **65**.

Rigid-rod peptide conjugates **66** self-assemble into rigid-rod β-barrel pores **67–72** (Fig. 8). New members of this family are pores **67**, **69**, **71** and **72**. In pore **69**, LWV-triads were positioned at the outer surface, instead of the uniform LLL-triads

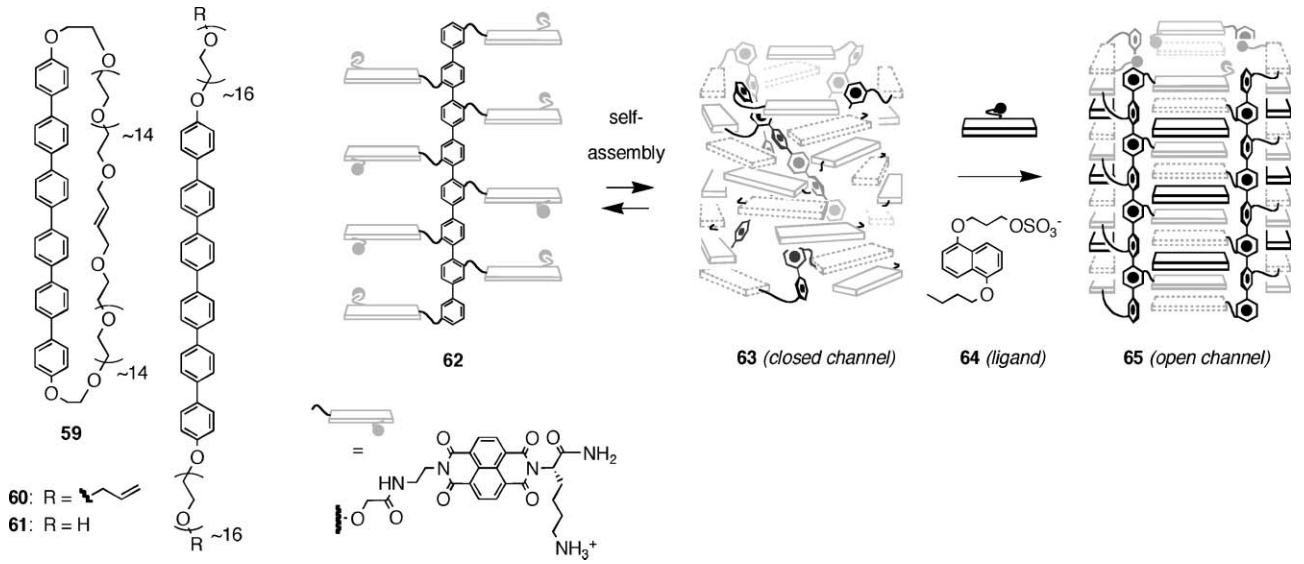

Fig. 7 Rigid *p*-oligophenyl rods in giant macrocycles (**59**) and as staves in ligand-gated barrel-stave ion channels **65** that open in response to the intercalation of π-donor ligands **64** into π-acceptor helix **63**.

of conventional rigid-rod β-barrels like homolog **68**, to modulate β-barrel stability as well as barrel–membrane interactions.[59] The formal external LLL → LWV mutation from the old pore **68**, with internal RH-dyads, to the new pore **69**, with an identical interior, shortened single-channel lifetimes from minutes to milliseconds and increased Hill coefficients from n = 0.6 to n = 3.7. These changes demonstrated that pore **69** is tetrameric, unstable and labile,

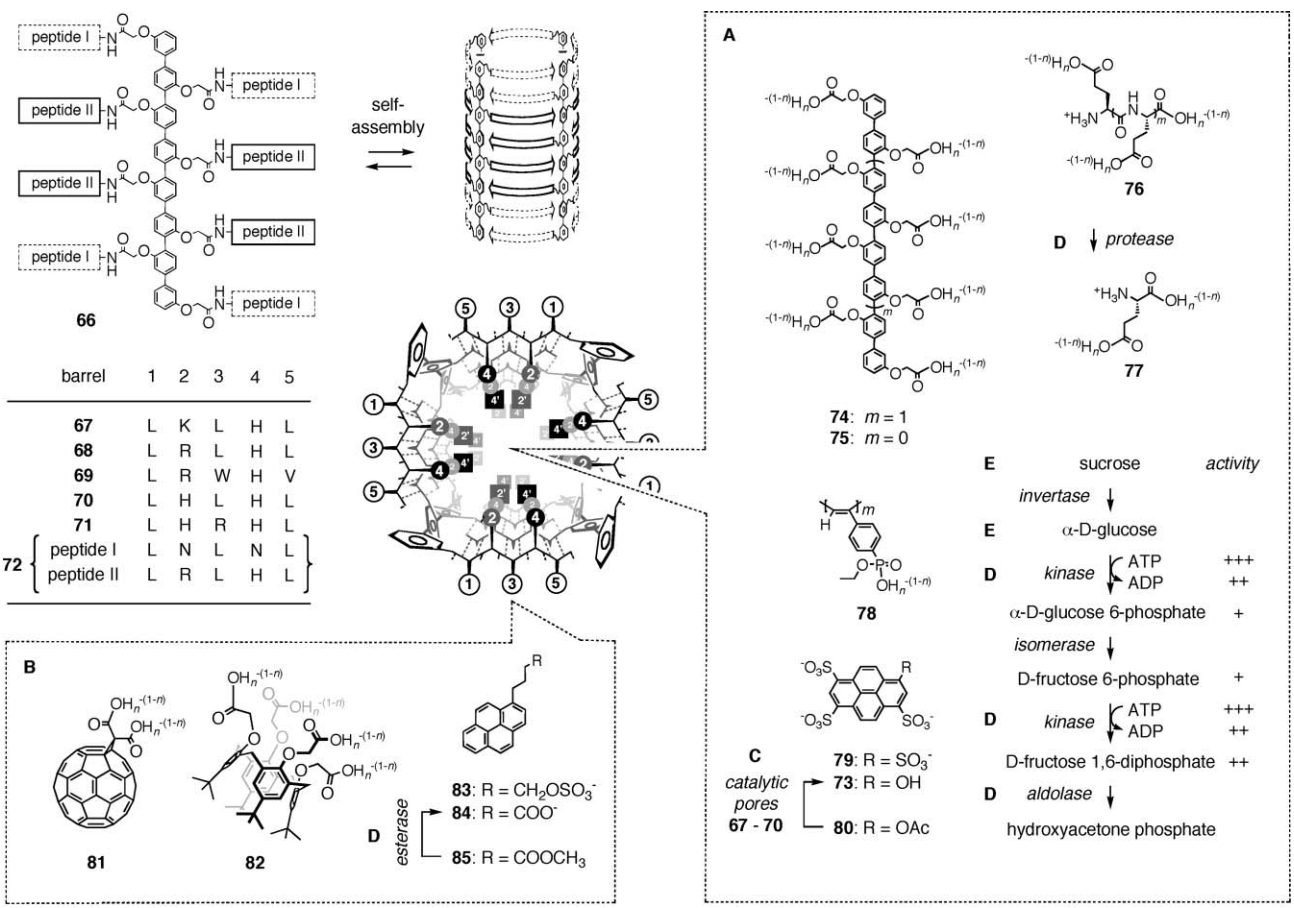

Fig. 8 Synthetic multifunctional pores **67–72** with blockers (**A**) and ligands (**B**) and applications as catalysts (**C**, substrate **80**), transducers of (enzymatic) reactions into color (**D**), and sensors (sucrose, glucose, **E**).

whereas pore **68** is stable and inert. Fluorescence depth quenching demonstrated poor partitioning as well as transmembrane *p*-octiphenyl orientation. The latter finding supported the presence of barrel-stave rather than micellar pores despite poor kinetic stability. Moreover, it demonstrated the dominance of the transmembrane preference of hydrophobically matching rigid-rods over the interfacial preference of W (compare section 2). The identical interiors of RH-pores **68** and **69** were reflected in identical multifunctionalities, including pH gating, inversion of anion/cation selectivity at pH $\sim$ 5 (pH 4: $P_{Cl^-}/P_{K^+} = 3.8$, pH 6: $P_{Cl^-}/P_{K^+} = 0.5$) and blockage with 8-hydroxy-1,3,6-pyrene trisulfonate **73** (IC_{50} = 30 μM).

Rigid-rod pore **67** contains KH-dyads at the inner, and LLL-triads at the outer, barrel-surface.[60] The parabolic pH-profile, with maximal activity at pH 5, demonstrated double pH gating and suggested that full lysine and partial histidine protonation is needed to stabilize the internal space of pore **67**. The concentration dependence of 5(6)-carboxyfluorescein (CF) efflux from EYPC vesicles indicated the presence of thermodynamically unstable tetrameric barrel-stave supramolecules (n = 4.0). The long lifetime of high-conductance single pores in planar EYPC bilayers revealed ohmic single pores **67** that are inert and large (d = 12 Å). With the unstable and inert pore **67**, a complete set of thermodynamic and kinetic stabilities is available (**68**: stable, inert; **69**: unstable, labile; **70**: stable, labile).

Pore **67** could be blocked by representative guests in planar (**73**, IC_{50} = 190 μM, n = 4.9) and spherical bilayers. Rigid rods **74** and **75** were introduced as shape-persistent, dimeric (**74**: n = 2.0) α-helix mimics of poly-L-glutamic acid **76** (n = 1.0).[61] Comparison of their pH-profiles allowed the dissection of contributions from α-helix deprotonation and unfolding to pore blockage. The results provided experimental evidence for α-helix recognition by rigid-rod β-barrel pores. Blockage of biological pores such as melittin required more than 1000-times higher concentrations of poly-L-glutamic acid **76**.[62] The detection of the hydrolysis of poly-L-glutamic acid **76** into the inactive glutamate **77** was therefore possible with pore **67** but not with melittin. Polyene **78** was introduced as a CD-sensitive, shape-persistent α-helix-mimicking blocker (IC_{50} = 40 nM). Blocker **78** provided access to the imaging of pore-blocker complexes as single pseudo-rotaxanes by atomic force microscopy (AFM).[63] Analysis of the strikingly non-statistical AFM histograms revealed the mechanism of pore blockage as fast threading into preformed barrels **67** followed by slow translocation through the blocked and contracted pore. The efflux of the smaller blockers **73** through blocked pores **68** and its competitive inhibition with analog **79** was demonstrated to occur in spherical EYPC vesicles.[64] Blocker efflux through blocked ion channels and pores was proposed as a universal mechanism of selectivity, applicable also to biological potassium channels, protein translocators, and so on.

Different from the situation with RH-pore **69**, blockage of KH-pore **67** by adenosine triphosphate (ATP) and adenosine diphosphate (ADP) was sufficiently different to be detectable with the naked eye as a binary on/off signal.[65] ATP/ADP discrimination was used to detect the phosphorylation of glucose and fructose 6-phosphate by the corresponding kinases. The former system provided access to sugar sensing in soft drinks with pore **67**. To do so, soft drinks were treated first with invertase, and the conversion of the good blocker ATP into the poor blocker ADP during the subsequent phosphorylation of glucose and fructose was then detected as an increasing fluorescence emission due to the increasing activity of pore **67**.

Esterolytic activity of catalytic pore **67** showed saturation kinetics for a representative substrate (8-acetoxy-1,3,6-pyrene trisulfonate **80**, K_M = 0.6 μM). Hill plots demonstrated that the catalyst (like the pore) is a tetrameric supramolecule (n = 3.7). The dependence of the esterolytic activity of pores **67–70** on ionic strength was used for the non-invasive determination of structural and functional contributions of the surrounding bilayer.[66] Membrane sensitivity in salt-rate profiles decreased with increasing acidity of the functional groups at the internal pore surface (**68** $\sim$ **69** > **67** > **70**).

Rigid-rod {242}-barrels **72**, without a uniform β-strand sequence, were introduced to create synthetic pores with central and peripheral domains for voltage-sensitive molecular recognition.[67] Pore **72** contains a central domain with four "active" RH-dyads per β-strand at the inner barrel surface that is flanked by peripheral domains composed of two "inactive" NN-dyads each. This active-site contraction caused, compared to all-RH pore **68**, a four-fold reduction of pore activity (EC_{50} = 140 nM), a reduction of single pore lifetimes from minutes to seconds and a reduction of single pore homogeneity. Ohmic behavior, reasonably high conductance (d_{Hille} = 7.0 Å, consistent with counterion immobilization as in pore **68**) and pH gating around pH 5 remained unchanged. Increased molecular recognition of blockers such as phytate (IP_6) > ATP > ADP, despite active-site contraction in **72** compared to **68**, demonstrated that active-site location rather than size is important for function. Voltage-sensitive pore blockage was confirmed in polarized spherical and planar bilayers. Application of the Woodhull model revealed the depth of guest inclusion (also in vesicles). The found l_W = 10.4 Å for ADP blockage in planar EYPC bilayers was in agreement with the designed suprastructure of pore **72**.

In pore **71**, external design is introduced to provide access to ligand gating.[68,69] Without ligands, the external LRL-triads produce a hydrophilic outer pore surface and, therefore, inactivity because of a lacking partitioning into lipid bilayers. Molecular recognition of the external guanidinium arrays by amphiphilic argininophiles (fullerene **81** (EC_{50} = 10 nM) > calixarene **82** > pyrenes **83** > **84**) increases external lipophilicity to improve partitioning and therefore activates the pore. Compared to classical pores **67–70**, the presence of external ligands in pore **71** resulted in the disappearance of pH gating, the inhibition of intervesicular pore transfer and the appearance of flickering in the currents of single open pores. Internal α-helix recognition exemplified with poly-L-glutamic acid **76** caused noncompetitive blockage of ligand-gated pores **71**. Noncompetitive blockage was confirmed by independence of effective blocker concentration (IC_{50} = 45 nM) on varied effective ligand concentration (**82**: EC_{50} = 440 nM, **83**: EC_{50} = 3.3 μM, **84**: EC_{50} = 14.8 μM). Structural studies using FRET from *p*-octiphenyl donors in the pore to BODIPY acceptors in the bilayer and molecular mechanics simulations were in agreement with these interpretations. The hydrolysis of the

inactive substrate **85** with pig liver esterase into the active ligand **84** was detectable continuously as increasing fluorescence emission, that is activity of pore **71**, with increasing reaction time.

Cholate dimers **86** and **87** aggregate in planar lipid bilayers to form cation channels (Fig. 9).[70] Hydroxylated **86** showed two distinct single channel conductances of 9.5 and 25 pS (500 mM salt) with similar ion selectivities ($P_{K^+}/P_{Cl^-} \sim 7$, $P_{K^+}/P_{Na^+} \sim 2.5$). The methylated variant **87** showed variable conductances of 5–20 pS, with a greater cation selectivity ($P_{K^+}/P_{Cl^-} \sim 17$, $P_{K^+}/P_{Na^+} \sim 3$). These differences are attributed to the aggregation state of each channel, *i.e.* the number of staves per barrel. Trimeric and tetrameric suprastructures are proposed.

Molecular umbrellas **88–91** permeate POPC/POPG (95:5) vesicle membranes and deliver a reversibly bound 16-mer oligonucleotide cargo (dT_{16}) transmembrane (POPC/POPG: 1-palmitoyl-2-oleoyl phosphatidylcholine/1-palmitoyl-2-oleoyl phosphatidylglycerol).[71,72] The polar cargo is shielded from the hydrophobic membrane interior by the facially amphiphilic steroidal conjugate during transport. In this case the transported species is an integral part of the membrane-breaching structure with a mode of action somewhat between that of a carrier and a pore. Transport rates of tetracholamides **90** and **91** were an order of magnitude greater than those of bischolamides **88** and **89**. Removal of the 7-hydroxyl group from each cholamide had little effect on activity. Across mammalian cell mimicking cholesterol-rich membranes (POPC:POPG:cholesterol 65:5:30) transport rates for tetracholamides **90** and **91** were much improved, whilst no improvement was observed with the bischolamides.

Due to the facially amphiphilic nature of cholate, oligocholates **92–97** are thought to self-assembly into barrel-stave pores.[73] In Na NMR kinetics in spherical POPC membranes, oligocholates **94** and **95**, containing the rigid *p*-phenylenediamine, exhibit $n = 1$ concentration dependence. The more flexible variants **92**, **93**, **96** and **97** follow $n = 2$. The different Hill coefficients can be interpreted as a change from unimolecular to supramolecular barrel-stave channels or as a decrease in the thermodynamic stability of structurally identical supramolecular channels. The transport rates were unrelated to the Hill coefficients (**92** > **94** ~ **93** ~ **97** > **96** ~ **95**). Various persulfated analogues of this nature were synthesized and displayed activity as antiviral agents. The mechanism of action is unclear but these heavily charged variants were proved to retain the ability to traverse vesicle membranes.[74]

Dodecacholamide **92** and decacholamide **98** formed dimeric pores large enough to enable CF release from dipalmitoyl phosphatidylcholine (DPPC) vesicles at 43 °C, *i.e.*, in the liquid crystalline phase.[75] The release rate was largely retarded at 37 °C, where the rigidity of the DPPC lipids in the gel phase is believed to 'squeeze out' pores from the membrane. Hindered partitioning with reduced membrane fluidity occurs with most biological and synthetic ion channels and pores and cannot be used as an experimental indication for a carrier mechanism.

3.3 Complex minimalist systems

The smaller the molecular structure, the more complex the active, often transient suprastructures of synthetic ion channels and pores. Barrel-rosette or micellar motifs are usually expected, but structural data are in most cases not available and always very difficult to secure. Synthetic ion channels and pores formed by small molecules are referred to as complex minimalist systems for this reason.

Steroid polyether conjugates **99–103** were studied as synthetic cation channels in comparison with previously known active dimers **104** and **105** (Fig. 10).[76] According to Na NMR kinetics in spherical EYPC/EYPG membranes (EYPG: egg yolk phospatidylglycerol), the transport rates of

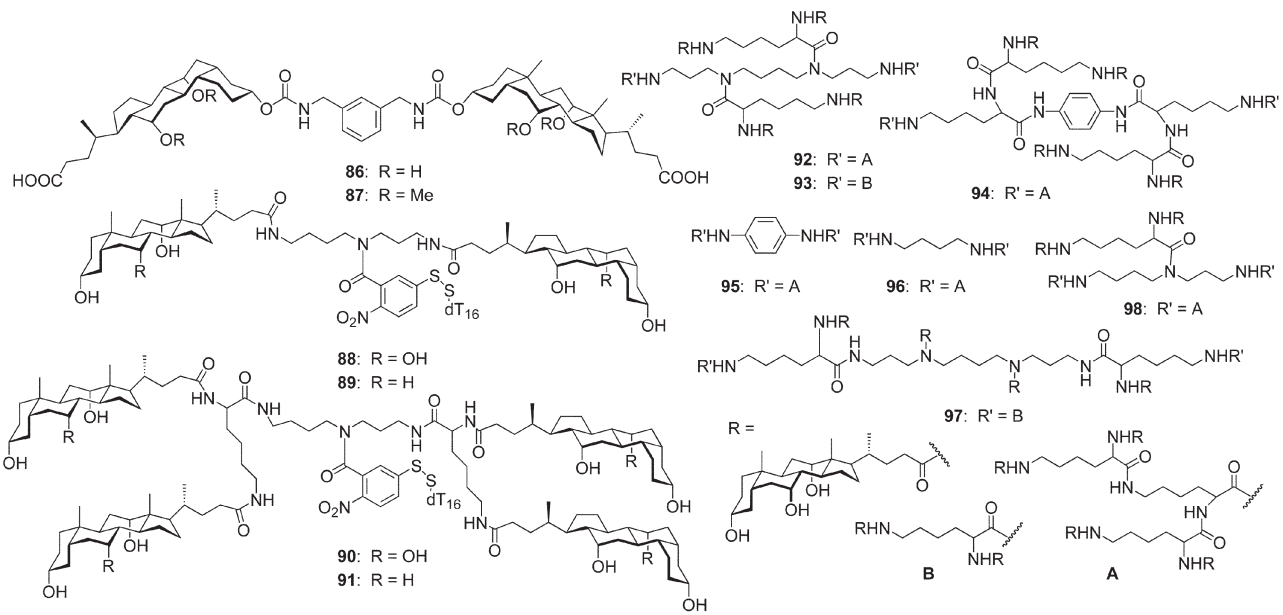

Fig. 9 Dimeric and oligomeric steroids that may act as carriers (**88–91**), barrel-stave ion channels (**86**, **87**, **92–97**) and/or transient micellar pores (**88–92**, **98**).

99 and **100** were akin to that of **104**. However, whereas covalent dimers **104** and **105** were also shown to transport protons across vesicle membranes, the monomeric series **99–103** were largely inactive towards this aim.

Anion selective transmembrane chloride influx across spherical POPC membranes was measured for cholates **106–108** using a chloride-sensitive fluorescent dye assay.[77] Transport rates increased with the measured binding strength of each receptor to chloride anions in chloroform (**106** < **107** < **108**) and were independent of cations present in the assay. Decreasing activity with decreasing membrane fluidity (DPPC) and inability to transport larger molecules like CF are compatible with a carrier mechanism but do not exclude the presence of ion channels. Related cationic cholates **109–111** were found to facilitate the translocation of anionic phospholipids from the inner leaflet of human erythrocytes to the outer surface thus mimicking the action of PS-scramblase enzymes involved in apoptosis (PS: phosphatidylserine).[78] 3-α amides **110** and **111** were less active than previously reported ester **109**.

Two cationic steroid antibiotics, the more active **112** and the less active **113**, were fluorescently labeled to elucidate the structural origin of their high selectivity for Gram-negative bacteria.[79] Reminiscent of the targeted pore formation of nisin in lipid II rich bacteria and amphotericin B in ergosterol rich fungi (see section 2), hexaamine **112** was found to bind specifically to lipid A, a dominant component of the plasma membrane of Gram-negative bacteria (K_D = 5.9 μM). The less potent tetraamine **113** was used to reveal that the affinity to Gram-negative bacteria exceeds that to Gram-positive bacteria by four orders of magnitude and that to eukaryotic cells by five orders of magnitude.

A library of amphiphilic steroid–peptide conjugates **114** was tested for antibacterial activity against Gram-negative *E. coli* and Gram-positive *Staphylococcus aureus*.[80] Six amino acids were used, histidine, lysine, methionine, phenylalanine, tryptophan and valine, falling into two categories of either basic or hydrophobic. Steroid **114**, with the arene-rich amino acid sequence FFK (compare section 2), showed the best minimum inhibitory concentrations.

Gating with light continues[36–41,1] to attract scientific attention, not only with regard to synthetic but also to bioengineered[81–83] ion channels and pores (compare section 3.1). EYPC liposomes containing artificial photoswitchable azo-dye based lipids **115** and **116** were shown to undergo photocontrolled calcein release.[84] This phenomenon was attributed to pore formation by photoisomerized *cis*-isomers as release rates increased greatly upon UV irradiation. Rates could be controlled by varying UV irradiation time and azo-lipid concentration. Steroidal **115** was less effective than acyclic **116**, possibly due to the membrane stabilising effect of cholesterol. Calcein efflux could effectively be switched on or off by light stimuli over several cycles.

Otherwise stable distearoyl phosphatidylcholine (DSPC) vesicles containing 5% of photocleavable lipid **117** were 'uncorked', releasing 6-carboxyfluorescein upon irradiation (Fig. 11).[85] Smooth release was observed following photolysis of the hydrophilic head group of **117**.

Amphiphilic β-diketones **118** and **119** were synthesized and studied as Eu^{III} binding units anchored within EYPC vesicles.[86] Transmembrane transport of Eu^{III} was observed and further monitored by exploiting the luminescent properties of Eu complexes. Metal ion transport was independent of membrane fluidity (DPPC).

Precedence suggests that ceramide forms giant barrel-rosette pores; recent reports indicate similar behavior for sphingosine.[87] Ceramide mimics **120–123** caused chloride and CF efflux from dioleoyl phosphatidylcholine/dioleoyl phosphatidic acid (DOPC/DOPA) 7:3 vesicles.[88] The chloride efflux

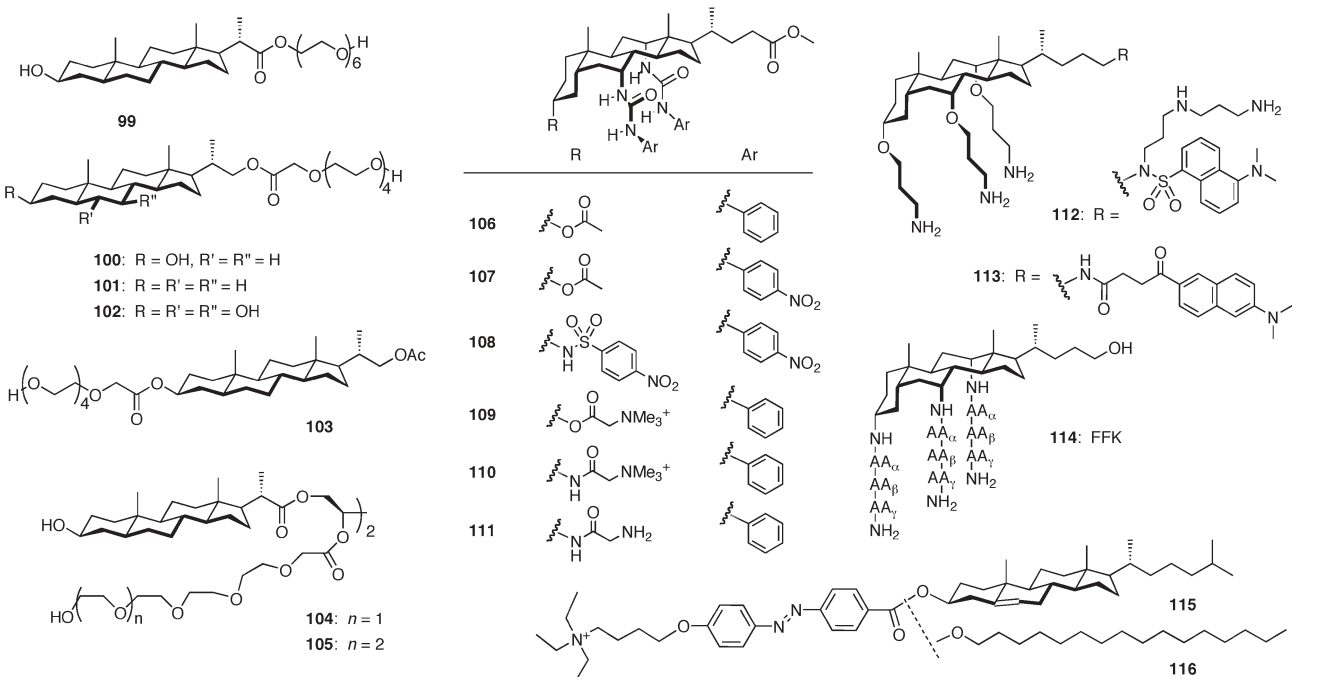

Fig. 10 Monomeric steroids that may act as carriers, barrel-rosette ion channels and/or transient micellar pores.

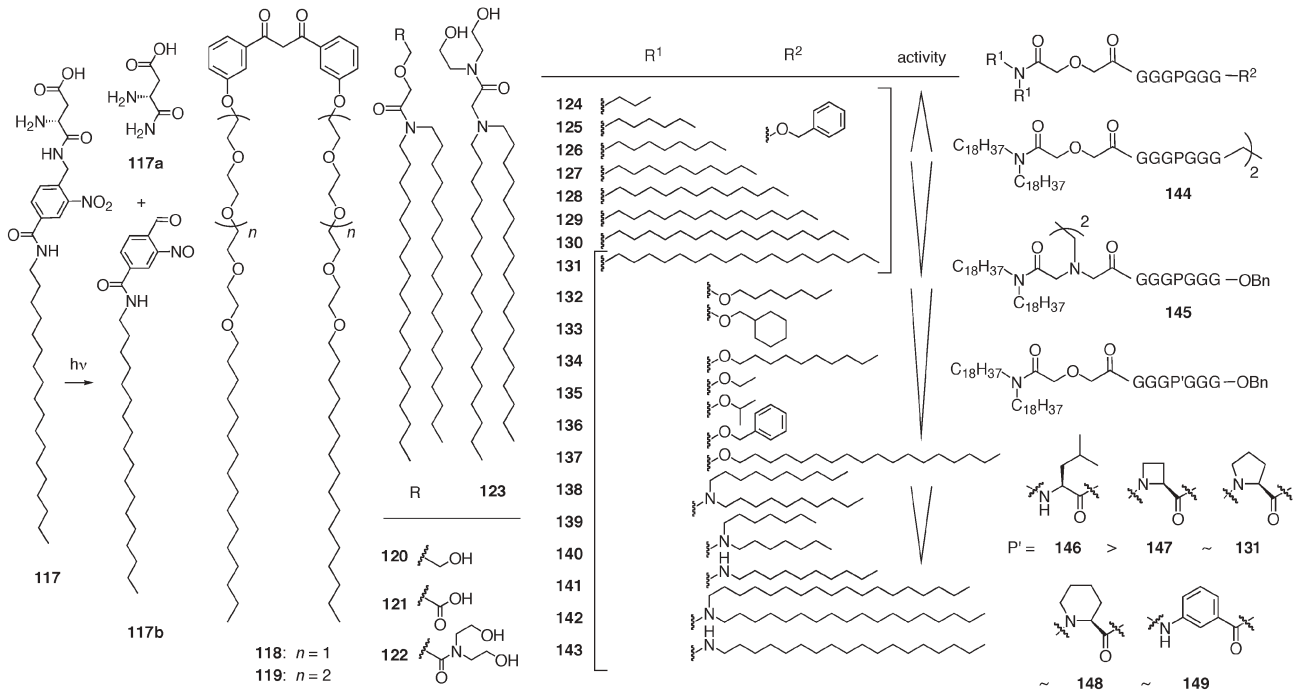

Fig. 11 Membrane-active single, double, triple and quadruple chain amphiphiles.

rates as measured by a selective electrode were modest yet followed the order **123** > **120** ~ ceramide (≫**121** ~ **122** = inactive). The order of CF efflux was **123** > **122** > **120**. Light scattering measurements showed that a large increase in vesicle diameter could be observed after addition of these model lipids. Facilitated vesicle fusion is the most plausible explanation.

Heptapeptide membrane lipid mimics of form **124–143** are known to transport chloride and CF anions across lipid bilayers.[89] The complexation of such receptors with chloride salts in $CDCl_3$ or CD_2Cl_2 was studied.[90] A systematic study measuring chloride and CF efflux from DOPC/DOPA 7:3 vesicles showed that activity is sensitive to the identity of hydrophobic membrane anchors at two opposing termini of the framework. The active dimer with an inner diameter $d \geqslant 8$ Å suggested by Hill plots and CF efflux was supported by increased chloride release with covalent dimers **144** > **145** compared to **131**.[91] Only minor differences in chloride and CF efflux rates were observed when replacing the proline residue in **131** with other cyclic amino acids and acyclic leucine (**146–149**).[92] A leucine derivative, however, in which the alkyl groups of the R^1 position are monodecyl-/monoethyl-substituted showed unusually high activity with $n = 4$.

3.4 Peptide mimics

Amphiphilic dipeptides containing one cationic arginine residue and a bulky hydrophobic synthetic residue of form **150** showed moderate antibacterial activity towards Gram-positive *S. aureus* and weaker activity towards Gram-negative *E. coli* (Fig. 12).[93] Dipeptide dendrimers **151** were obtained by peripheral modification of Aida's dipeptide dendrimer gelators.[94,95] In the solid state, dipeptide dendrimers **151** self-assembled into barrel-rosette-like suprastructures reminiscent of the established nanotubes formed by dipeptides such as diphenylalanine.[96] In an unusual assay, based on pH-sensitive porphyrins trapped in vesicles, dipeptides **151** fail to partition into lipid bilayers but may have some activity to mediate pH-gradient collapse. More data on function will be needed to understand the possible relevance of solid-state suprastructures for possible membrane activity.

A series of facially amphiphilic triarylamides of form **152** showed moderate antibacterial activities against *E. coli* and *S. aureus*.[97] Cation **153** was the most active. Calcein efflux from anionic PC/PS (9:1) vesicles was induced by **153** below antibacterial concentrations. Generally, active compounds also lysed human erythrocytes at around antibiotic concentrations. This undesirable property was closely correlated to the measured hydrophobicity of each species. Addition of a hydrophilic ethanolamine moiety to the central aryl unit decreased haemolysis without profoundly affecting activity such that **154** is highly selective for bacterial over mammalian membranes. Related facially amphiphilic arylurea oligomers **155** > **156** > **157** were approximately an order of magnitude more potent than arylamides **152** against *E. coli* and *B. subtilis* bacteria; selectivity for bacterial over mammalian cells was poor.[98]

Oligo-β-peptides **158** and **159** adopt 14-helical conformations (where helical periodicity is described by a 14-membered macrocycle) in various media with ring-constrained **159** even forming a stable 14-helix in water.[99] The 14-helix results in an amphiphilic structure with charged residues and hydrophobic residues separated on different faces of the chain. Both oligopeptides are potent antibiotics akin to the naturally occurring class of amphiphilic cationic host-defence peptides. CD studies indicated that interactions between oligo-β-peptides and anionic lipid bilayers serve to induce helicity,

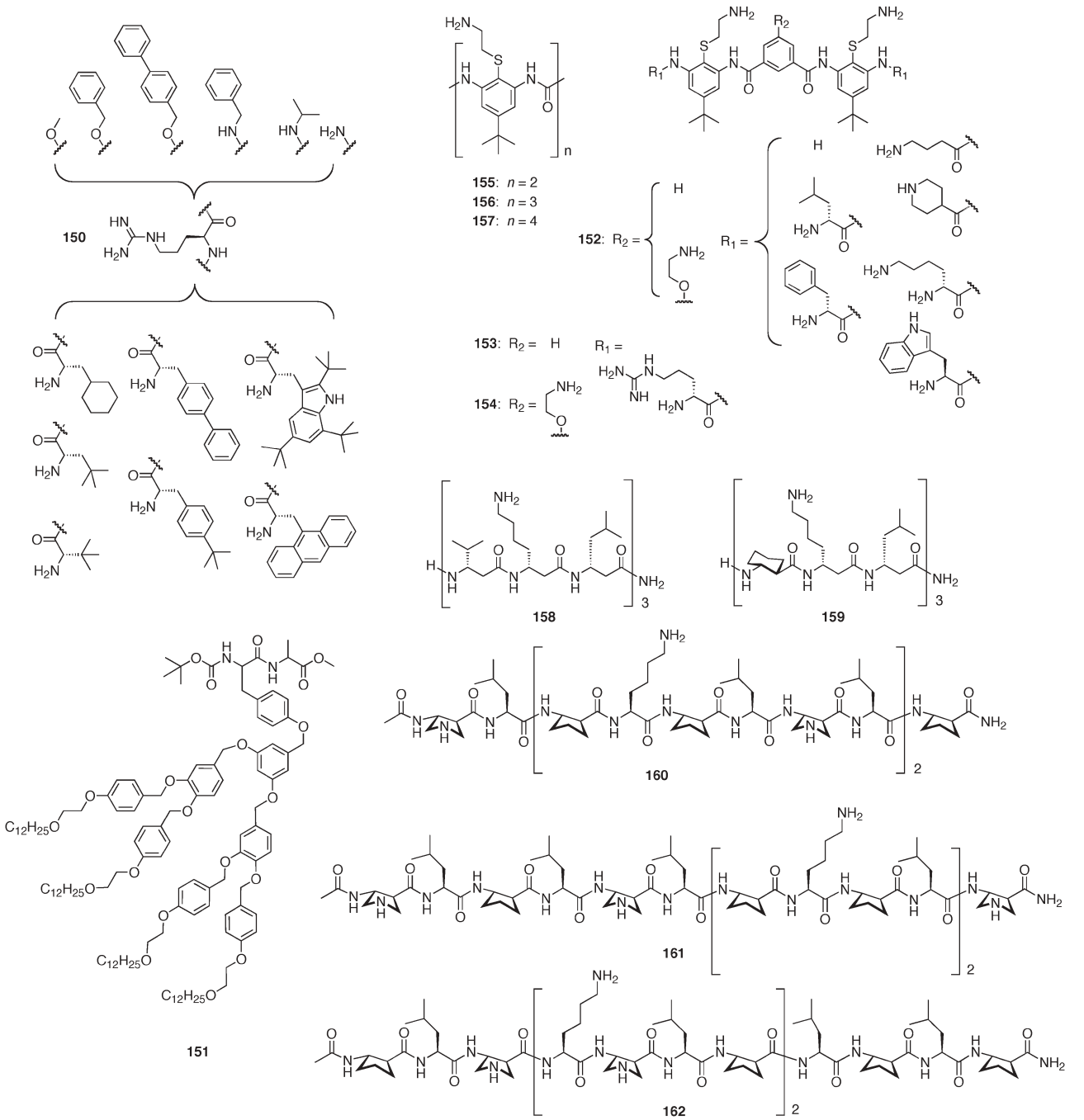

Fig. 12 Membrane-active peptide mimics.

consistent with findings that **158** (less inherent helix forming propensity) and **159** have comparable bactericidal activity. Both oligopeptides caused dye leakage (ANTS: 8-amino-naphthalene-1,3,6-trisulfonate) with greater effects observed from vesicles containing anionic phospholipids (DOPC/DOPG > DOPE/DOPG > DOPC) (DOPE: dioleoyl phosphatidylethanolamine. DOPA: dioleoyl phosphatidic acid). Consistent with the formation of micellar pores, oligopeptides **158** and **159** caused significant phospholipid flip-flop and exhibited fusogenic activity.

Oligopeptides **160–162** with mixed α- and β-residues are expected to form 14/15-helical structures with mixed periodicity.[100] However, global amphiphilicity can still result from designed side chain positioning, as with **160** and **161**. Oligopeptide **162** has a sequence that disallows global amphiphilicity in 14/15-helix conformation. In a departure from perceived wisdom, peptide **162**, with scrambled residues, showed high potency against several bacteria and was generally more active and more selective for prokaryotic cells than **161**.

A combinatorial approach was employed to synthesize families of oligo-β-peptides expected to adopt globally amphiphilic 12-helical conformations.[101] Libraries of 12-mers containing acyclic and cyclic, lipophilic and charged residues

(as with **158–162** above) were tested for antibacterial ability. The most promising sequences were expanded to 16-mer series. Many active 16-mers were found, although not with improved potency compared to previous best compounds. There appears to be a lower limit on minimum inhibitory concentration which is believed to be related to the mechanism of action.

3.5 Synthetic polymers

Cationic polymers derived from units **163–165** were investigated as host-defence mimics (Fig. 13).[102] Poly-**163** with an average molecular weight near 3000 (*cf.* magainin M_w = 2478) exhibited moderate antibacterial activity, without discrimination between bacteria and erythrocytes. Copolymers of **163** with up to 20% **164** showed slightly improved activity, whilst poly-**165** was inactive.

Amphiphilic polymers derived from cationic norbornene units **166–169** were found to disrupt liposomal membranes and were tested for antibacterial activity.[103,104] Various narrowly polydisperse poly-**166** (*PDI* = 1.17–1.30) of differing molecular weight facilitated calcein efflux from bacterial membrane mimicking anionic vesicles (PC:PS = 9:1). Membrane disrupting activity increased with molecular weight, up to a maximum plateau at above 4 500 g mol^{-1}. Mammalian cell membrane mimicking neutral vesicles of cholesterol/PC were significantly more stable towards disruption. Antibacterial and non-haemolytic properties could be tailored by controlling the degree of hydrophobicity. Copolymers containing 10% **166** (high antibiotic activity) and 90% **168** (non-haemolytic) retained the desirable features of each constituent (activity: **169** ~ **166** > **168** ≫**167**, selectivity: **169** ~ **168** ≫ **168** ~ **167**).

Polyphenylene ethynylenes **170–172** and polyarylamide **173** show facially amphiphilic conformations in solution, in the solid state and at the oil–water interface.[105,106] Their antibacterial potency against a broad range of Gram-positive and Gram-negative bacteria was assayed. The most hydrophobic pentoxy-substituted **170** was inactive. 20-mer **171** was highly active but lysed erythrocytes at antibiotic concentrations. Hexamer **172** showed a higher selectivity for bacterial over mammalian cells but had reduced activity. Polymeric films of **172** showed promising behavior as antifouling coatings.

Three series of amphiphilic random copolymers **174–176** with varying degrees of polymerization and mole percentages of hydrophobic butyl residues (from 0 to 60%) were tested for antibacterial activity against *E. coli*.[107] Modest activities were measured. The most promising series was the shorter chain **176**. Increasing the proportion of hydrophobic residues decreased activity and lowered selectivity for bacterial over mammalian erythrocytes (haemolysis).

Various copolymers of **177** and **178** units (M_w = 10 000–50 000), bearing acidic and basic groups, were synthesized.[108]

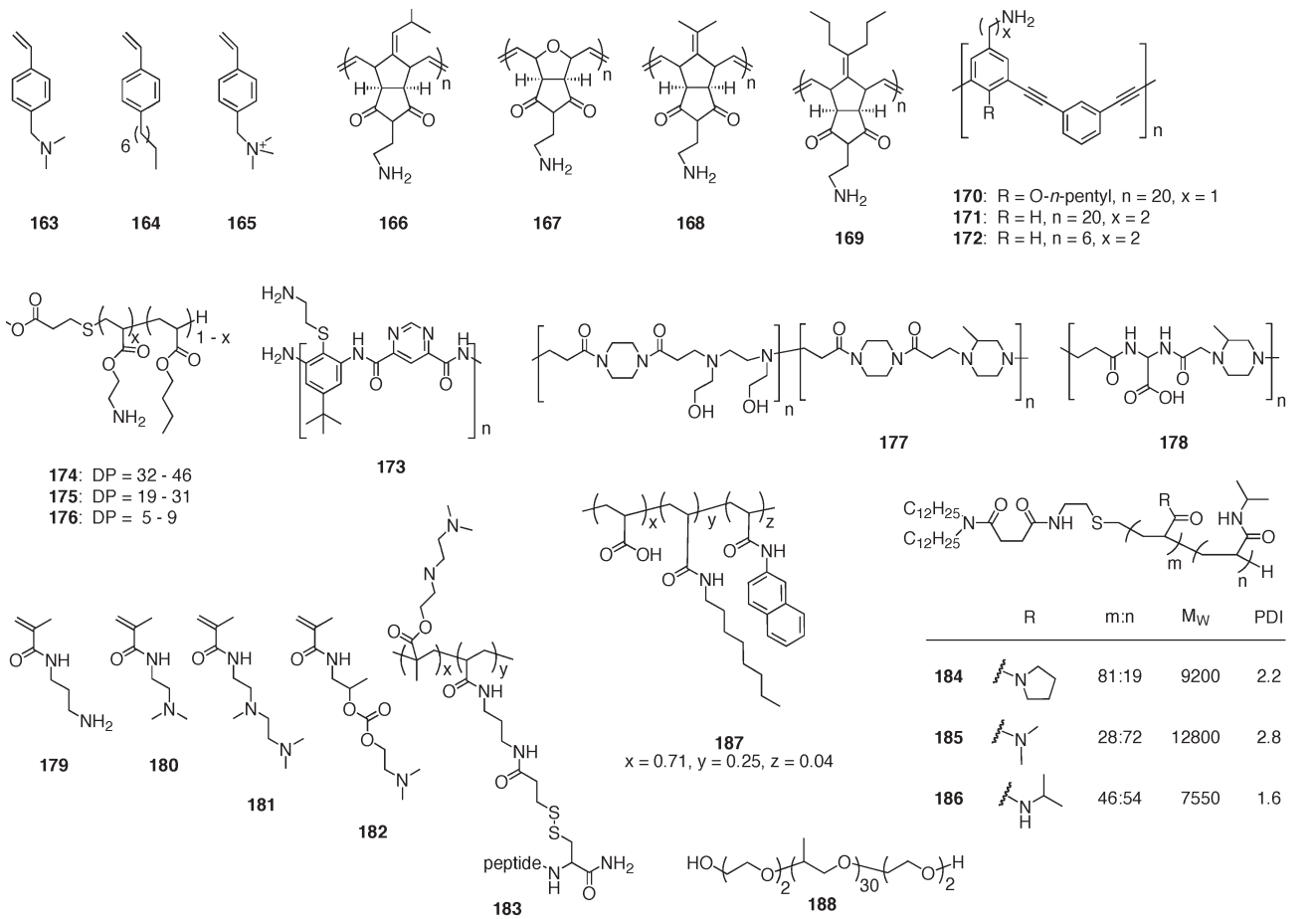

Fig. 13 Membrane-active synthetic polymers.

Their haemolytic activity decreased with increasing pH from pH 5.5 (active) to pH 7.4 (inactive). Copolymers of amine **179** enriched with amines **180–182** (95:5 ratio) were prepared (M_w = 100 000–400 000).[109] The peptides in poly-**183** were introduced by modification of poly-**179** residues after copolymerization. Efficient calcein release from EYPC/cholesterol 2:1 vesicles was observed due to such polymers at pH 5.0 but much diminished effects were observed at pH 7.4. Under acidic conditions, the peptide unit underwent a conformational change from random coil to α-helix as measured by circular dichroism spectroscopy.

Copolymers **184–186** were modified with a hydrophobic tail for anchoring in EYPC liposomes.[110] Facilitated calcein release was observed. Release rates increased with temperature from negligible transport at 25 °C to 90%, 30% and 10% release in 5 min at 42 °C with **186** > **185** > **184**, respectively. Above 30–40 °C such polymers are known to undergo a conformational transition from hydrophilic to hydrophobic, in this case resulting in membrane permeabilization.

The amphiphilic polymer **187** facilitated calcein leakage from EYPC/DPPA vesicles with a rate highly dependent on the ionic strength (transport increased with increasing NaCl concentration).[111] Full vesicle fragmentation occurred after prolonged incubation time.

The triblock copolymer of poly(ethylene oxide) and poly(propylene oxide) **188** increased cation permeability of planar lipid bilayers.[112] Depending on conditions, the conductance characteristics observed signified that three modes of action could exist: detergent-like, carrier or single channel (compare section 1). Higher order aggregation was required to form mildly cation-selective ion channels (K^+ > Ca^{2+} > *N*-methylglucamine). The current–voltage dependence was not linear for single channels, with current flow increasing disproportionately with increased current.

4 Epilogue

During the last two years, it has been exciting to see several new groups embarking on research in the field of synthetic ion channels and pores. The overall appreciable productivity yielded stimulating contributions to a by now rich collection of synthetic ion channels and pores. For future progress, it will be important to further minimize the distractions of nonproductive mechanistic and structural controversies and, more importantly, to maximize efforts to create ambitious functions "beyond the simple hole." This shift of attention will be essential for the successful implementation of the expected practical applications of synthetic ion channels and pores as drugs (antibiotics), drug delivery vehicles, catalysts, detectors and sensors. Meaningful contributions in this direction will be of critical importance for continuing growth, appreciation and credibility of an exciting and overall still underexplored field.

Acknowledgements

This work was supported by the Swiss NSF (SM) and the Higher Education Commission of Pakistan (MRS). SB is a fellow of the Roche Research Foundation.

References

1 S. Matile, A. Som and N. Sordé, *Tetrahedron*, 2004, **60**, 6405–6435.
2 S. Matile and N. Sakai, in *Analytical Supramolecular Chemistry*, ed. C. Schalley, Wiley Weinheim, in preparation.
3 N. Sakai and S. Matile, *Chem. Biodiversity*, 2004, **1**, 28–43.
4 N. Sakai and S. Matile, *J. Phys. Org. Chem.*, 2006, **19**, DOI: 10.1002/poc.1047.
5 S. Khademi, J. O'Connell, III, J. Remis, Y. Robles-Colmenares, L. J. W. Miercke and R. M. Stroud, *Science*, 2004, **305**, 1587–1594.
6 B. A. Krantz, R. A. Melnyk, S. Zhang, S. J. Juris, D. B. Lacy, Z. Wu, A. Finkelstein and R. J. Collier, *Science*, 2005, **309**, 777–781.
7 X. Guan, L.-Q. Gu, S. Cheley, O. Braha and H. Bayley, *ChemBioChem*, 2005, **6**, 1875–1881.
8 Y. Astier, H. Bayley and S. Howorka, *Curr. Opin. Chem. Biol.*, 2005, **9**, 576–584.
9 S. H. White and G. von Heijne, *Curr. Opin. Struct. Biol.*, 2005, **15**, 378–386.
10 F. Perret, M. Nishihara, T. Takeuchi, S. Futaki, A. N. Lazar, A. W. Coleman, N. Sakai and S. Matile, *J. Am. Chem. Soc.*, 2005, **127**, 1114–1115.
11 H. E. Hasper, B. de Kruijff and E. Breukink, *Biochemistry*, 2004, **43**, 11567–11575.
12 I. Wiedemann, R. Benz and H.-G. Sahl, *J. Bacteriol.*, 2004, **186**, 3259–3261.
13 X. X. Li, B. Davis, V. Haridas, J. U. Gutterman and M. Colombini, *Biophys. J.*, 2005, **88**, 2577–2584.
14 T. Yamaguchi, S. Tashiro, M. Tominaga, M. Kawano, T. Ozeki and M. Fujita, *J. Am. Chem. Soc.*, 2004, **126**, 10818–10819.
15 M. G. J. ten Cate, M. Crego-Calama and D. N. Reinhoudt, *J. Am. Chem. Soc.*, 2004, **126**, 10840–10841.
16 J. T. Davis, *Angew. Chem., Int. Ed.*, 2004, **43**, 668–698.
17 Z. Siwy, L. Trofin, P. Kohli, L. A. Baker, C. Trautmann and C. R. Martin, *J. Am. Chem. Soc.*, 2005, **127**, 5000–5001.
18 C. C. Harrell, P. Kohli, Z. Siwy and C. R. Martin, *J. Am. Chem. Soc.*, 2004, **126**, 15646–15647.
19 Y. Kobuke, K. Ueda and M. Sokabe, *Chem. Lett.*, 1995, 435–436.
20 T. M. Fyles, D. Loock and X. Zhou, *J. Am. Chem. Soc.*, 1998, **120**, 2997–3003.
21 N. Sakai, C. Ni, S. M. Bezrukov and S. Matile, *Bioorg. Med. Chem. Lett.*, 1998, **8**, 2743–2747.
22 C. Goto, M. Yamamura, A. Satake and Y. Kobuke, *J. Am. Chem. Soc.*, 2001, **123**, 12152–12159.
23 N. Sakai, D. Gerard and S. Matile, *J. Am. Chem. Soc.*, 2001, **123**, 2517–2524; N. Sakai and S. Matile, *J. Am. Chem. Soc.*, 2002, **124**, 1184–1185.
24 N. Sakai, D. Houdebert and S. Matile, *Chem.–Eur. J.*, 2003, **9**, 223–232.
25 N. Sakai, B. Baumeister and S. Matile, *ChemBioChem*, 2000, **1**, 123–125.
26 N. Sakai and S. Matile, *Chem. Commun.*, 2003, **38**, 2514–2523.
27 N. Sakai, J. Mareda and S. Matile, *Acc. Chem. Res.*, 2005, **38**, 79–87.
28 M. Majumder, N. Chopra and B. J. Hinds, *J. Am. Chem. Soc.*, 2005, **127**, 9062–9070.
29 M. Majumder, N. Chopra, R. Andrews and B. J. Hinds, *Nature*, 2005, **438**, 44.
30 I. Tabushi, Y. Kuroda and K. Yokota, *Tetrahedron Lett.*, 1982, **23**, 4601–4604.
31 N. Madhavan, E. C. Robert and M. S. Gin, *Angew. Chem., Int. Ed.*, 2005, **44**, 7584–7587.
32 L. Bacri, A. Benkhaled, P. Guégan and L. Auvray, *Langmuir*, 2005, **21**, 5842–5846.
33 Y. J. Jeon, H. Kim, S. Jon, N. Selvapalam, D. Y. Oh, I. Seo, C.-S. Park, S. R. Jung, D.-S. Koh and K. Kim, *J. Am. Chem. Soc.*, 2004, **126**, 15944–15945.
34 N. Maulucci, F. De Riccardis, C. B. Botta, A. Casapullo, E. Cressina, M. Fregonese, P. Tecilla and I. Izzo, *Chem. Commun.*, 2005, 1354–1356.
35 W.-H. Chen, M. Nishikawa, S.-D. Tan, M. Yamamura, A. Satake and Y. Kobuke, *Chem. Commun.*, 2004, 872–873.

36 P. Shum, J.-M. Kim and D. H. Thompson, *Adv. Drug Delivery Rev.*, 2001, **53**, 273–284.
37 R. H. Bisby, C. Mead and C. G. Morgan, *Biochem. Biophys. Res. Commun.*, 2000, **276**, 169–173.
38 Y. Kobuke and A. Ohgoshi, *Colloids Surf., A*, 2000, **169**, 187–197.
39 B. Bondurant, A. Mueller and D. F. O'Brien, *Biochim. Biophys. Acta*, 2001, **1511**, 113–122.
40 L. Husaru, R. Schulze, G. Steiner, T. Wolf, W. D. Habicher and R. Salzer, *Anal. Bioanal. Chem.*, 2005, **382**, 1882–1888.
41 L. Husaru, M. Gruner, T. Wolff, W. D. Habicher and R. Salzer, *Tetrahedron Lett.*, 2005, **46**, 3377–3379.
42 O. V. Yarishkin, A. K. Tashmukhamedova, U. Z. Mirkhodjaev and B. A. Tashmukhamedov, *J. Inclusion Phenom. Macrocyclic Chem.*, 2004, **49**, 139–144.
43 W. M. Leevy, M. E. Weber, M. R. Gokel, G. B. Hughes-Strange, D. D. Daranciang, R. Ferdani and G. W. Gokel, *Org. Biomol. Chem.*, 2005, **3**, 1647–1652.
44 A. Nakano, Q. Xie, J. V. Mallen, L. Echegoyen and G. W. Gokel, *J. Am. Chem. Soc.*, 1990, **112**, 1287–1289.
45 G. W. Gokel, P. H. Schlesinger, N. K. Djedovic, R. Ferdani, E. C. Harder, J. Hu, W. M. Leevy, J. Pajewska, R. Pajewski and M. E. Weber, *Bioorg. Med. Chem.*, 2004, **12**, 1291–304.
46 M. E. Weber, P. H. Schlesinger and G. W. Gokel, *J. Am. Chem. Soc.*, 2005, **127**, 636–642.
47 W. M. Leevy, M. E. Weber, P. H. Schlesinger and G. W. Gokel, *Chem. Commun.*, 2005, **40**, 89–91.
48 W. M. Leevy, S. T. Gammon, T. Levchenko, D. D. Daranciang, O. Murillo, V. Torchilin, D. Piwnica-Worms, J. E. Huettner and G. W. Gokel, *Org. Biomol. Chem.*, 2005, **3**, 3544–3550.
49 A. E. Meyer, W. M. Leevy, R. Pajewski, I. Suzuki, M. E. Weber and G. W. Gokel, *Bioorg. Med. Chem.*, 2005, **13**, 3321–3327.
50 W. M. Leevy, M. R. Gokel, G. B. Hughes-Strange, P. Schlesinger and G. W. Gokel, *New J. Chem.*, 2005, **29**, 205–209.
51 W. M. Leevy, J. E. Huettner, R. Pajewski, P. H. Schlesinger and G. W. Gokel, *J. Am. Chem. Soc.*, 2004, **126**, 15747–15753.
52 J. Srinivas, C. F. Lopez and M. L. Klein, *J. Phys. Chem. B*, 2004, **108**, 4231–4235.
53 C. F. Lopez, S. O. Nielsen, P. B. Moore and M. L. Klein, *Proc. Natl. Acad. Sci. U. S. A.*, 2004, **101**, 4431–4434.
54 C. F. Lopez, S. O. Nielsen, B. Ensing, P. B. Moore and M. L. Klein, *Biophys. J.*, 2005, **88**, 3083–3094.
55 E. Biron, F. Otis, J.-C. Meillon, M. Robitaille, J. Lamothe, P. Van Hove, M.-E. Cormier and N. Voyer, *Bioorg. Med. Chem.*, 2004, **12**, 1279–1290.
56 W.-Y. Yang, J.-H. Ahn, Y.-S. Yoo, N.-K. Oh and M. Lee, *Nat. Mater.*, 2005, **4**, 399–402.
57 P. Talukdar, G. Bollot, J. Mareda, N. Sakai and S. Matile, *J. Am. Chem. Soc.*, 2005, **127**, 6528–6529.
58 P. Talukdar, G. Bollot, J. Mareda, N. Sakai and S. Matile, *Chem.–Eur. J.*, 2005, **11**, 6525–6532.
59 P. Talukdar, N. Sakai, N. Sordé, D. Gerard, V. M. F. Cardona and S. Matile, *Bioorg. Med. Chem.*, 2004, **12**, 1325–1336.
60 S. Litvinchuk, G. Bollot, J. Mareda, A. Som, D. Ronan, M. R. Shah, P. Perrottet, N. Sakai and S. Matile, *J. Am. Chem. Soc.*, 2004, **126**, 10067–10075.
61 S. Litvinchuk and S. Matile, *Supramol. Chem.*, 2005, **17**, 135–139.
62 N. Sordé and S. Matile, *Biopolymers*, 2004, **76**, 55–65.
63 J. Kumaki, E. Yashima, G. Bollot, J. Mareda, S. Litvinchuk and S. Matile, *Angew. Chem., Int. Ed.*, 2005, **44**, 6154–6157.
64 D. Ronan, N. Sordé and S. Matile, *J. Phys. Org. Chem.*, 2004, **17**, 978–982.
65 S. Litvinchuk, N. Sordé and S. Matile, *J. Am. Chem. Soc.*, 2005, **127**, 9316–9317.
66 A. Som and S. Matile, *Chem. Biodiversity*, 2005, **2**, 717–729.
67 Y. Baudry, D. Pasini, M. Nishihara, N. Sakai and S. Matile, *Chem. Commun.*, 2005, 4798–4800.
68 V. Gorteau, F. Perret, G. Bollot, J. Mareda, A. N. Lazar, A. W. Coleman, D.-H. Tran, N. Sakai and S. Matile, *J. Am. Chem. Soc.*, 2004, **126**, 13592–13593.
69 V. Gorteau, G. Bollot, J. Mareda, D. Pasini, D.-H. Tran, A. N. Lazar, A. W. Coleman, N. Sakai and S. Matile, *Bioorg. Med. Chem.*, 2005, **13**, 5171–5180.
70 M. Yoshii, M. Yamamura, A. Satake and Y. Kobuke, *Org. Biomol. Chem.*, 2004, **2**, 2619–2623.
71 B. Jing, V. Janout, B. C. Herold, M. E. Klotman, T. Heald and S. L. Regen, *J. Am. Chem. Soc.*, 2004, **126**, 15930–15931.
72 V. Janout, B. Jing and S. L. Regen, *J. Am. Chem. Soc.*, 2005, **127**, 15862–15870.
73 W.-H. Chen, X.-B. Shao and S. L. Regen, *J. Am. Chem. Soc.*, 2005, **127**, 12727–12735.
74 B. Jing, V. Janout, B. C. Herold, M. E. Klotman, T. Heald and S. L. Regen, *J. Am. Chem. Soc.*, 2004, **126**, 15930–15931.
75 W.-H. Chen and S. L. Regen, *J. Am. Chem. Soc.*, 2005, **127**, 6538–6539.
76 E. Avallone, E. Cressina, M. Fregonese, P. Tecilla, I. Izzo and F. De Riccardis, *Tetrahedron*, 2005, **61**, 10689–10698.
77 B. A. McNally, A. V. Koulov, B. D. Smith, J.-B. Joos and A. P. Davis, *Chem. Commun.*, 2005, 1087–1089.
78 K. M. DiVittorio, T. N. Lambert and B. D. Smith, *Bioorg. Med. Chem.*, 2005, **13**, 4485–4490.
79 B. Ding, N. Yin, Y. Liu, J. Cardenas-Garcia, R. Evanson, T. Orsak, M. Fan, G. Turin and P. B. Savage, *J. Am. Chem. Soc.*, 2004, **126**, 13642–13648.
80 B. Ding, U. Taotofa, T. Orsak, M. Chadwell and P. B. Savage, *Org. Lett.*, 2004, **6**, 3433–3436.
81 T. Loughbreed, V. Borisenko, T. Hennig, K. Rück-Braun and G. A. Wooley, *Org. Biomol. Chem.*, 2004, **2**, 2798–2801.
82 M. Banghart, K. Borges, E. Isacoff, D. Trauner and R. H. Kramer, *Nat. Neurosci.*, 2004, **7**, 1381–1386.
83 A. Kocer, M. Walko, W. Meijberg and B. L. Feringa, *Science*, 2005, **309**, 755–758.
84 X.-M. Liu, B. Yang, Y.-L. Wang and J.-Y. Wang, *Chem. Mater.*, 2005, **17**, 2792–2795.
85 B. Chandra, S. Mallik and D. K. Srivastava, *Chem. Commun.*, 2005, 3021–3023.
86 V. Marchi-Artzner, M.-J. Brienne, T. Gulik-Krzywicki, J.-C. Dedieu and J.-M. Lehn, *Chem.–Eur. J.*, 2004, **10**, 2342–2350.
87 L. J. Siskind, S. Fluss, M. Bui and M. Colombini, *J. Bioenerg. Biomembr.*, 2005, **37**, 227–236.
88 R. Pajewski, N. Djedovic, E. Harder, R. Ferdani, P. H. Schlesinger and G. W. Gokel, *Bioorg. Med. Chem.*, 2005, **13**, 29–37.
89 N. Djedovic, R. Ferdani, E. Harder, J. Pajewska, R. Pajewski, M. E. Weber, P. H. Schlesinger and G. W. Gokel, *New J. Chem.*, 2005, **29**, 291–305.
90 R. Pajewski, R. Ferdani, P. H. Schlesinger and G. W. Gokel, *Chem. Commun.*, 2004, 160–161.
91 R. Pajewski, R. Ferdani, J. Pajewska, N. Djedovic, P. H. Schlesinger and G. W. Gokel, *Org. Biomol. Chem.*, 2005, **3**, 619–625.
92 R. Ferdani, R. Pajewski, N. Djedovic, J. Pajewska, P. H. Schlesinger and G. W. Gokel, *New J. Chem.*, 2005, **29**, 673–680.
93 B. E. Haug, W. Stenson, T. Stiberg and J. S. Svendsen, *J. Med. Chem.*, 2004, **47**, 4159–4162.
94 W.-D. Jang, D.-L. Jiang and T. Aida, *J. Am. Chem. Soc.*, 2000, **122**, 3232–3233.
95 V. Percec, A. E. Dulcey, V. S. Balagurusamy, Y. Miura, J. Smidrkal, M. Peterca, S. Nummelin, U. Edlund, S. D. Hudson, P. A. Heiney, H. Duan, S. N. Magonov and S. A. Vinogradov, *Nature*, 2004, **430**, 764–768.
96 M. Yemini, M. Reches, E. Gazit and J. Rishpon, *Anal. Chem.*, 2005, **77**, 5155–5159.
97 D. Liu, S. Choi, B. Chen, R. J. Doerksen, D. J. Clements, J. D. Winkler, M. L. Klein and W. F. DeGrado, *Angew. Chem., Int. Ed.*, 2004, **43**, 1158–1162.
98 H. Tang, R. J. Doerken and G. N. Tew, *Chem. Commun.*, 2005, 1537–1539.
99 R. F. Epand, T. L. Raguse, S. H. Gellman and R. M. Epand, *Biochemistry*, 2004, **43**, 9527–9535.
100 M. A. Schmitt, B. Weisblum and S. H. Gellman, *J. Am. Chem. Soc.*, 2004, **126**, 6848–6849.
101 E. A. Porter, B. Weisblum and S. H. Gellman, *J. Am. Chem. Soc.*, 2005, **127**, 11516–11529.
102 M. A. Gelman, B. Weisblum, D. M. Lynn and S. H. Gellman, *Org. Lett.*, 2004, **6**, 557–560.
103 M. F. Ilker, H. Schule and E. B. Coughlin, *Macromolecules*, 2004, **37**, 694–700.
104 M. F. Ilker, K. Nüsslein, G. N. Tew and E. B. Coughlin, *J. Am. Chem. Soc.*, 2004, **126**, 15870–15875.

105 J. Rennie, L. Arnt, H. Tang, K. Nüsslein and G. N. Tew, *J. Ind. Microbiol. Biotechnol.*, 2005, **32**, 296–300.
106 L. Arnt, K. Nüsslein and G. Tew, *J. Polym. Sci., Part A: Polym. Chem.*, 2004, **42**, 3860–3864.
107 K. Kuroda and W. F. DeGrado, *J. Am. Chem. Soc.*, 2005, **127**, 4128–4129.
108 N. Lavignac, M. Lazenby, P. Foka, B. Malgesini, I. Verpilio, P. Ferruti and R. Duncan, *Macromol. Biosci.*, 2004, **4**, 922–929.
109 A. M. Funhoff, C. F. van Nostrum, M. C. Lok, J. A. W. Kruijtzer, D. J. A. Crommelin and W. E. Hennink, *J. Controlled Release*, 2005, **101**, 233–246.
110 K. Yoshino, A. Kadowaki, T. Takagishi and K. Kono, *Bioconjugate Chem.*, 2004, **15**, 1102–1109.
111 F. Vial, S. Rabhi and C. Tribet, *Langmuir*, 2005, **21**, 853–862.
112 O. O. Krylova and P. Pohl, *Biochemistry*, 2004, **43**, 3696–3703.